Inclusion-Induced Bilayer Deformations: Effects of Monolayer Equilibrium Curvature

Claus Nielsen*† and Olaf S. Andersen*

*Department of Physiology and Biophysics, Cornell University, Weill Medical College, New York, New York 10021 USA, and †August Krogh Institute, University of Copenhagen, Copenhagen DK-2100, Denmark

ABSTRACT The energetics of protein-induced bilayer deformation in systems with finite monolayer equilibrium curvature were investigated using an elastic membrane model. In this model the bilayer deformation energy ΔG_{def} has two major components: a compression-expansion component and a splay-distortion component, which includes the consequences of a bilayer curvature frustration due to a monolayer equilibrium curvature, c_0, that is different from zero. For any choice of bilayer material constants, the value of ΔG_{def} depends on global bilayer properties, as described by the bilayer material constants, as well as the energetics of local lipid packing adjacent to the protein. We introduce this dependence on lipid packing through the contact slope, s, at the protein-bilayer boundary. When $c_0 = 0$, ΔG_{def} can be approximated as a biquadratic function of s and the monolayer deformation at the protein/bilayer boundary, u_0: $\Delta G_{def} = a_1 u_0^2 + a_2 u_0 s + a_3 s^2$, where a_1, a_2, and a_3 are functions of the bilayer thickness, the bilayer compression-expansion and splay-distortion moduli, and the inclusion radius (this expression becomes exact when the Gaussian curvature component of ΔG_{def} is negligible). When $c_0 \neq 0$, the curvature frustration contribution is determined by the choice of boundary conditions at the protein-lipid boundary (by the value of s), and ΔG_{def} is the sum of the energy for $c_0 = 0$ plus the curvature frustration-dependent contribution. When the energetic penalty for the local lipid packing can be ignored, ΔG_{def} will be determined only by the global bilayer properties, and a $c_0 > 0$ will tend to promote a local inclusion-induced bilayer thinning. When the energetic penalty for local lipid packing is large, s will be constrained by the value of c_0. In a limiting case, where s is determined only by geometric constraints imposed by c_0, a $c_0 > 0$ will impede such local bilayer thinning. One cannot predict curvature effects without addressing the proper choice of boundary conditions at the protein-bilayer contact surface.

INTRODUCTION

Lipid bilayers are self-assembled structures of amphipathic molecules with material properties similar to those of smectic liquid crystals (Helfrich, 1973; Evans and Hochmuth, 1978). Changes in bilayer shape (lipid packing) therefore will incur an energetic cost (Helfrich, 1973, 1981). This is important because the hydrophobic bilayer-spanning domains of integral membrane proteins (Deisenhofer et al., 1985; Henderson et al., 1990; Doyle et al., 1998) couple the proteins to the surrounding bilayer (Owicki et al., 1978). Consequently, when membrane proteins undergo conformational changes that involve the protein-lipid boundary (Unwin and Ennis, 1984; Unwin, 1995; Kaback and Wu, 1997; Sakmar, 1998; Perozo et al., 1998), the structure of the surrounding bilayer will be perturbed, and the free energy difference between two protein conformations will vary with the difference in bilayer deformation energy associated with the different bilayer perturbations (Gruner, 1991). The bilayer deformation energies can be evaluated using the theory of elastic liquid-crystal deformations (Huang, 1986), and, because the bilayer mechanical properties vary as a function of the lipid composition (Evans and Needham, 1987; Needham, 1995), the energetics of bilayer-protein interactions provide for a mechanism by which the bilayer lipid composition can be a determinant of protein conformation and function.

The bilayer component of biological membranes contains lipids that in isolation form nonbilayer structures (Luzzati and Husson, 1962) (see Epand (1997) for a recent summary), and isolated lipid monolayers at equilibrium may be nonplanar—they may have a curvature (Cullis and deKruijff, 1979; Gruner, 1985; Seddon, 1990; Lundbæk et al., 1997; Andersen et al., 1999). This propensity to form nonbilayer structures is likely to be important. First, many cells regulate their bilayer lipid composition such that optimal cell growth occurs close to, but below, the bilayer→nonbilayer phase transition temperature (Lindblom et al., 1993; Rilfors et al., 1993; Rietveld et al., 1993) (see Hazel (1995) for a recent summary). Second, changes in monolayer equilibrium curvature modulate the function of many integral membrane proteins (cf. Epand (1997) for a review), as well as well-defined model systems (Keller et al., 1993; Lundbæk and Andersen, 1994; Bezrukov et al., 1995, 1998; Lundbæk et al., 1996), suggesting that the monolayer equilibrium curvature could be a modulator of biological function (Gruner, 1985; Hui, 1997).

The monolayer equilibrium curvature is determined by the effective "shapes" of the monolayer-forming lipids, which in turn are determined by the variation of the lateral stress or pressure profile $t(z)$ through the monolayer (see Fig. 1 *a*). For an isolated, planar monolayer at equilibrium,

Received for publication 28 October 1999 and in final form 5 July 2000.

Address reprint requests to Dr. Claus Nielsen, Department of Zoophysiology, August Krogh Institute, University of Copenhagen, Universitetsparken 13, DK-2100 Copenhagen. Tel.: 45-35-32-16-47; Fax: 45-35-32-15-67; E-mail: clnielsen@aki.ku.dk.

0006-3495/00/11/2583/22 $2.00

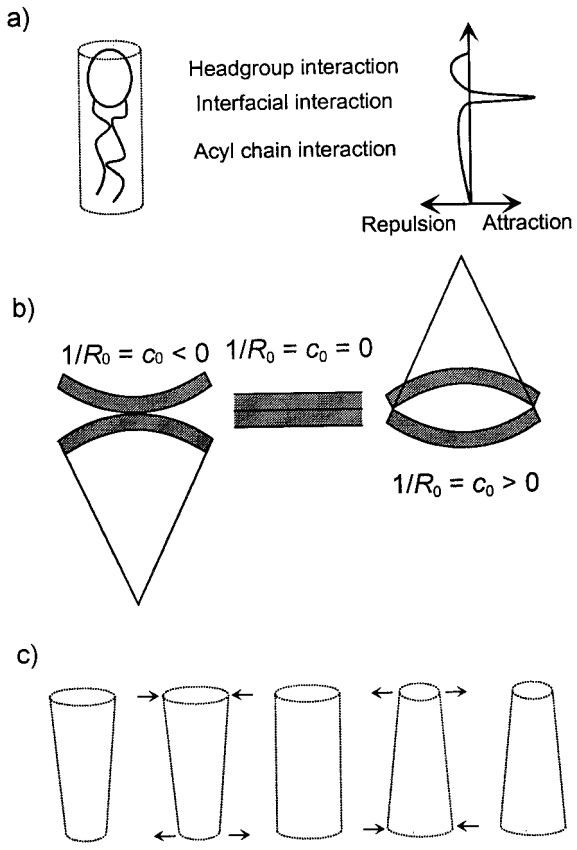

FIGURE 1 Intermolecular forces, lipid shape, monolayer curvature, and bilayer stress. (*a*) Effective lipid shape (*left*) together with intermolecular interactions (*center*) determines the lateral pressure profile in a monolayer (*right*). (*b*) The spontaneous radius of curvature R_0 together with an (arbitrary) assignment of a surface normal determines the monolayer equilibrium curvature c_0. (*c*) Monolayers with equilibrium curvature $c_0 \neq 0$ change their effective lipid molecular shape from cones to cylinders to form a (frustrated) planar bilayer.

the integral of the profile $t(z)$ over the monolayer thickness is zero (Seddon, 1990), and the average molecular shape of the lipids is cylindrical. If the (unperturbed) lipid molecules are not cylindrical, the positive and negative stresses are not symmetrical about a neutral surface (a surface where the area does not change with changes in monolayer curvature; Rand et al., 1990; Templer et al., 1994), and there will be a bending moment, or torque, around this surface. A nonzero bending moment means that the monolayer will tend to curve away from a planar geometry, toward its equilibrium curvature c_0 (Fig. 1 *b*).

Whatever the monolayer equilibrium curvature, the two monolayers must adapt to one another to form a bilayer. In the case of symmetrical bilayers, the bilayer curvature will be zero. Thus, for lipid molecules that form curved monolayers, the adaptation involves a change in the effective lipid shape, from noncylindrical to cylindrical (Seddon, 1990) (Fig. 1 *c*). This change in shape means that energy is stored in the bilayer—the so-called *curvature frustration energy* (Gruner, 1985; Sadoc and Charvolin, 1986). Inclusions (lipids or proteins) that perturb the bilayer will alter the local energy density; conversely, inclusions may be affected by the deformation energy, which will affect protein function (Andersen et al., 1999).

THEORY

Continuum analyses of bilayer configurations are based on the concept of bilayer elasticity. Any planar bilayer configuration is endowed with a potential (elastic) energy. A change in bilayer configuration causes a reversible change in energy, and configurations with the lowest energy are the most likely to occur. The symbols used in this article are defined in Table 1.

Formulating the model

A length mismatch between the thickness of the hydrophobic core of an unperturbed bilayer, d_0, and the length, l, of the hydrophobic exterior surface of a bilayer inclusion, an integral membrane protein, will introduce an elastic deformation of the bilayer in the vicinity of the inclusion (Fig. 2 *a*). When the strength of the hydrophobic interactions between the bilayer-spanning part of the protein and the bilayer core is strong enough to ensure that there is no exposure of hydrophobic residues to water, when there is strong hydrophobic coupling (Andersen et al., 1999), the bilayer deformation at the inclusion/bilayer boundary will be $d_0 - l$.

The ensuing bilayer deformation energy arises from contributions due to changes in bilayer thickness (with an associated energy density $K_a(2u/d_0)^2$, where K_a is the compression-expansion modulus and u is the local perturbation in monolayer thickness) and changes in monolayer curvature (with an associated energy density $K_c(c_1 + c_2 - c_0)^2/2$, where K_c is the mean splay distortion modulus and c_1 and c_2 are the principal monolayer curvatures) (Helfrich, 1973; Huang, 1986) (Fig. 2 *b*). In addition to these major contributions, there are two minor contributions: a surface-tension term, which previous analyses have shown to be negligible (Huang, 1986; Helfrich and Jakobsson, 1990; Nielsen et al., 1998), and a Gaussian curvature energy term with associated energy density $\overline{K_c}(c_1c_2)^2/2$, which also is negligible (see Appendix).

Besides the above energy contributions, there also may be an energetic cost associated with packing the lipids in immediate contact with the inclusion, which arises because the presence of the inclusion will decrease the range of motion of the bilayer lipids (Chiu et al., 1991, 1999; Woolf and Roux, 1996). The total deformation energy therefore is

$$\Delta G_{\text{def}} = \Delta G_{\text{continuum}} + \Delta G_{\text{packing}}, \qquad (1)$$

TABLE 1 List of symbols

Symbol	Meaning	Unit
R_{Head}	Effective lipid headgroup radius	nm
$t(z)$	Lateral pressure profile	pN/nm^2
K_a	Area compression-expansion modulus	pN/nm
K_c	Mean splay-distortion modulus	pN nm
$\overline{K}_c$	Gaussian splay-distortion modulus	pN nm
u	Monolayer perturbation	nm
u_0	Monolayer deformation at inclusion-bilayer boundary	nm
r	Radial distance from inclusion symmetry axis	nm
r_0	r at inclusion-bilayer boundary	nm
r_∞	Radial distance in the limit where $u(r) = 0$	nm
d_0	Equilibrium bilayer thickness	nm
l	Hydrophobic length of inclusion	nm
l_o	Hydrophobic length of model protein in the open state	nm
l_c	Hydrophobic length of model protein in the closed state	nm
s	Contact slope at inclusion-bilayer boundary	
s_{min}	Relaxed contact slope when $\partial\Delta G_{def}/\partial s = 0$	
c_0	Monolayer equilibrium curvature	nm^{-1}
c_1,c_2	Principal curvatures	nm^{-1}
$\Delta G_{def,c_0=0}$	Total deformation energy for $c_0 = 0$	kT
ΔG_{def}	Total deformation energy	kT
ΔG_{CE}	Nominal compression-expansion energy component	kT
ΔG_{SD}	Nominal splay-distortion energy component	kT
ΔG_{MEC}	Nominal monolayer equilibrium curvature energy	kT
ΔG_{GC}	Nominal Gaussian curvature energy component	kT
H_B	Bilayer spring constant	kT/nm^2
a_i	Coefficients in the quadratic expression for $\Delta G_{def,c=0}$	See Table 5
a_i^{CE}	Coefficients in the quadratic expression for $\Delta G_{CE,c=0}$	See Table 6
a_i^{SD}	Coefficients in the quadratic expression for $\Delta G_{SD,c=0}$	See Table 7
$n_{a,i}$, $n_{c,i}$, $n_{d,i}$, $n_{r,i}$	Exponents for the a_i's in the scaling relations	
$\bar{a}_{a,i}$, $\bar{a}_{c,i}$, $\bar{a}_{d,i}$, $\bar{a}_{r,i}$	Multiplicative coefficients for the scaling relations	See Tables 5–7
$\hat{a}_{a,i}$, $\hat{a}_{c,i}$, $\hat{a}_{d,i}$, $\hat{a}_{r,i}$	Additive coefficients for the scaling relations	See Tables 5–7

where $\Delta G_{continuum}$ is the continuum contribution to ΔG_{def}, due to the $K_a(2u_0/d_0)^2/2$ and $K_c(c_1 + c_2 - c_0)^2/2$ energy densities, and $\Delta G_{packing}$ denotes the (local) energetic cost due to the inclusion-induced packing constraints, which we will incorporate through the choice of boundary conditions used to solve the continuum problem.

In the case of uniform single component bilayers that are symmetrical about an unperturbed bilayer midplane, the continuum contribution to the bilayer deformation energy induced by a cylindrical inclusion with radius r_0 is obtained by integrating the energy densities over the perturbed area:

$$\begin{aligned}\Delta G_{continuum} &= \frac{1}{2}\int_{r_0}^{\infty}\left(K_a\left(\frac{2u}{d_0}\right)^2 + K_c(c_1 + c_2 - c_0)^2\right)2\pi r\,dr \\ &\quad - \frac{1}{2}\int_{r_0}^{\infty} K_c c_0^2\, 2\pi r\,dr \\ &= \pi\int_{r_0}^{\infty}\left(K_a\left(\frac{2u}{d_0}\right)^2 + K_c(c_1 + c_2)^2 - 2K_c(c_1 + c_2)c_0\right)r\,dr,\end{aligned} \tag{2}$$

where $K_c c_0^2/2$ is the curvature frustration energy density in the unperturbed bilayer. The material constants, K_a and K_c, have been determined in "macroscopic" continuum measurements (Evans and Hochmuth, 1978; Evans et al., 1995); it is not clear, however, whether these values are appropriate for describing bilayer deformations (cf. Helfrich, 1981).

To solve Eq. 2, which also will establish the deformation profile, one needs four boundary conditions. The first two are straightforward, as they describe the unperturbed bilayer far from the inclusion:

$$u(\infty) = 0 \tag{3a}$$

and

$$\left.\frac{\partial u}{\partial r}\right|_{\infty} = 0, \tag{3b}$$

where $u(r)$ denotes the monolayer perturbation as a function of r. The last two boundary conditions describe the perturbed bilayer at the inclusion/bilayer boundary and are subject to uncertainty.

For the third boundary condition, we assume that there is strong hydrophobic coupling, in which case the initial monolayer deformation u_0, at $r = r_0$, will be determined by

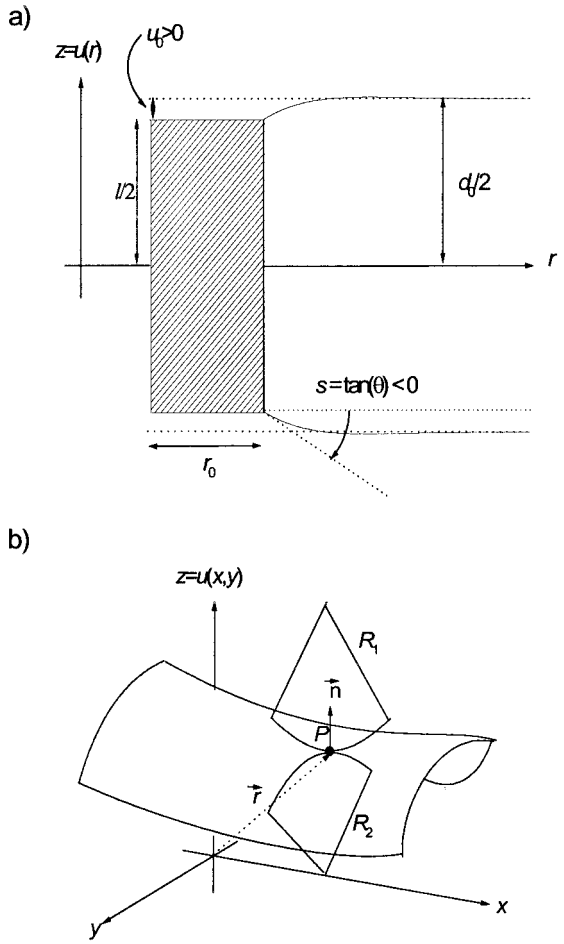

FIGURE 2 Inclusion-induced bilayer deformations and local curvature. (*a*) When $d_0 \neq l$, hydrophobic matching at the inclusion/bilayer boundary will cause the two monolayers to bend and thin or thicken, which gives rise to a bilayer deformation energy. For symmetrical bilayers and symmetrical cylindrical deformations, the problem can be reduced to a radially varying deformation of a monolayer with an unperturbed thickness $d_0/2$, where $z = u(r)$ denotes the perturbation in monolayer thickness at distance r from the inclusion axis. At the inclusion/bilayer boundary (at r_0), the deformation is u_0. The slope of the deformation at the contact surface, $du/dr|_{r_0}$, is denoted by s. (*b*) Local curvature. The position of a point P on the surface is given by $\vec{r} = (x, y, u(x, y))$; the associated area element normal is $\vec{n}$. The two directors whose curvatures are extrema are the principal directions; the corresponding principal curvatures are $c_1 = 1/R_1$ and $c_2 = 1/R_2$.

the mismatch between l and d_0:

$$u_0 = u(r_0) = \frac{d_0 - l}{2}. \tag{3c}$$

Equation 3c will not hold generally, as the bilayer deformation may be so large that the incremental change in the deformation energy may exceed the energetic penalty for exposing hydrophobic residues to water (Andersen et al., 1999; Lundbæk and Andersen, 1999).

The energetic consequences of lipid packing adjacent to the inclusion are introduced through the choice of the fourth boundary condition. If $\Delta G_{packing} = 0$, then $\Delta G_{def} = \Delta G_{continuum}$, and the minimum value of $\Delta G_{continuum}$ is attained when (Landau and Lifshitz, 1986)

$$\nabla^2 u|_{r_0} = 0, \tag{3d}$$

or, equivalently, when $\partial \Delta G_{continuum}/\partial s = 0$, where $s = \partial u/\partial r|_{r_0}$. That is, if one can neglect any molecular detail at the inclusion/lipid boundary, then s will relax toward the value for which $\Delta G_{continuum}$ is a minimum (Helfrich and Jakobsson, 1990), which we denote by $s = s_{min}$. We refer to Eq. 3d as the relaxed boundary condition and use the superscript rel whenever Eq. 3d applies.

The liquid-crystalline characteristics of lipid bilayers generally will make $\Delta G_{packing} \neq 0$, in which case it is necessary to introduce molecular detail to describe the constraints on the lipid packing (Ring, 1996). Given the known variation of $\Delta G_{continuum}$ with s (Huang, 1986; Helfrich and Jakobsson, 1990), we introduce the lipid packing constraints by constraining the value of s. For example, if a rigid cylindrical inclusion is imbedded in a bilayer composed of effectively cylindrical molecules, s will be close to zero because there can be no voids in the bilayer core at the lipid-protein boundary. We therefore choose the fourth boundary condition to be

$$\left.\frac{\partial u}{\partial r}\right|_{r_0} = 0 \quad \text{or} \quad s = 0. \tag{3e}$$

This boundary condition is in concordance with experimental results on the variation in gramicidin channel lifetime with bilayer thickness (Huang, 1986; Lundbæk and Andersen, 1999). Its physical significance is that the acyl chain movement adjacent to the inclusion will be constrained (cf. Chiu et al., 1999). If the lipid molecules in successive rings around the inclusion were free to slide relative to each other, the acyl chains in each monolayer would tilt with respect to the monolayer surface, and the lipid director would no longer be parallel to the surface normal, or $s \neq 0$. In the limit where the energetic penalty for tilt vanishes, s will become equal to s_{min}.

If the lipid shape is changed, from cylindrical to cone-shaped, but the penalty for tilt remains, a void-free alignment of the lipids around a cylindrical inclusion would mean that

$$\left.\frac{\partial u}{\partial r}\right|_{r_0} = \tan(\arcsin(R_{Head}c_0)) \approx R_{Head}c_0 \quad \text{for} \quad R_{Head}c_0 \ll 1, \tag{3f}$$

where R_{head} is the effective radius of the lipid headgroup. Equation 3f is an approximation, as it is assumed that the inclusion, or the inclusion-induced bilayer deformation, does not perturb the lipid shape. Accepting this, Eq. 3f is accurate to within 1% for $-0.3 \leq R_{head}c_0 \leq 0.3$. (Equation 3e describes the special case where $c_0 = 0$.) We refer to Eq.

3f as the constrained boundary condition, and use the superscript con whenever Eq. 3f applies. (One can similarly assign the value of $\partial u/\partial r|_{r_0}$ for noncylindrical inclusions.)

Because of the uncertainties about the lipid packing around an inclusion, which has an impact on the choice of s, we examine how ΔG_{def} varies for different choices of s.

Solution to the model

Examination of Eq. 2 shows that $\Delta G_{continuum}$, which from now on is equivalent to ΔG_{def} (subject to the value of s), is composed of two terms that formally are independent of c_0 and a term that explicitly depends on c_0. This distinction between (formally) c_0-dependent and c_0-independent terms becomes useful when the solution to the problem is formulated, as it turns out to be advantageous to evaluate separately the value of ΔG_{def} for $c_0 = 0$, which will be denoted $\Delta G_{def,c_0=0}$, and then add the explicitly c_0-dependent contribution.

When $c_0 = 0$ the bilayer deformation energy can be written as

$$\Delta G_{def,c_0=0} = \Delta G_{CE,c_0=0} + \Delta G_{SD,c_0=0}, \tag{4}$$

where $\Delta G_{CE,c_0=0}$ is the compression-expansion component

$$\Delta G_{CE,c_0=0} = \pi K_a \int_{r_0}^{\infty} \left(\frac{2u}{d_0}\right)^2 r\, dr \tag{5}$$

and $\Delta G_{SD,c_0=0}$ is the splay-distortion component

$$\Delta G_{SD,c_0=0} = \pi K_c \int_{r_0}^{\infty} (c_1 + c_2)^2 r\, dr. \tag{6}$$

(The c_1c_2-dependent (or Gaussian curvature) term is negligible compared to the other c_0-independent terms (see Appendix).) The c_0-dependent term in Eq. 2 depends on the fourth boundary condition only and can be written in closed form (Ring, 1996):

$$\begin{aligned}\Delta G_{MEC} &= -2\pi K_c c_0 \int_{r_0}^{\infty} (c_1 + c_2) r\, dr \\ &= -2\pi K_c c_0 \int_{r_0}^{\infty} \left(\frac{1}{r}\frac{\partial u}{\partial r} + \frac{\partial^2 u}{\partial r^2}\right) r\, dr \\ &= 2\pi K_c c_0 r_0 s.\end{aligned} \tag{7}$$

Combining Eqs. 4–7, ΔG_{def} can be written as

$$\begin{aligned}\Delta G_{def} &= \Delta G_{def,c_0=0} + \Delta G_{MEC} \\ &= \Delta G_{CE,c_0=0} + \Delta G_{SD,c_0=0} + \Delta G_{MEC}.\end{aligned} \tag{8}$$

The general solution to Eq. 4 is quadratic in u_0 and s (Nielsen et al., 1998):

$$\Delta G_{def,c_0=0} = a_1 u_0^2 + a_2 u_0 s + a_3 s^2, \tag{9}$$

where the coefficients a_1, a_2, and a_3 are functions of the mechanical moduli (K_a and K_c), r_0 and d_0, the parameters that describe the bilayer-inclusion system (scaling relations that allow these coefficients to be determined for any choice of K_a, K_c, r_0, and d_0 will be described in the Results section). Not only $\Delta G_{def,c_0=0}$, but also the component energies ($\Delta G_{CE,c_0=0}$ and $\Delta G_{SD,c_0=0}$) are biquadratic functions of u_0 and s:

$$\Delta G_{CE,c_0=0} = a_1^{CE} u_0^2 + a_2^{CE} u_0 s + a_3^{CE} s^2 \tag{10a}$$

and

$$\Delta G_{SD,c_0=0} = a_1^{SD} u_0^2 + a_2^{SD} u_0 s + a_3^{SD} s^2, \tag{10b}$$

which is important when evaluating the various contributions to ΔG_{def}.

For the constrained boundary condition and $c_0 = 0$, $s = 0$ and

$$\Delta G_{def,c_0=0}^{con} = a_1 u_0^2. \tag{11a}$$

The bilayer deformation energy thus is equivalent to the energy stored in a linear spring, and it is convenient to define a bilayer spring constant as

$$H_B^{con} = a_1/4. \tag{11b}$$

For the relaxed boundary condition and $c_0 = 0$, $\partial \Delta G_{def,c_0=0}/\partial s = 0$ and

$$s_{min} = \frac{-a_2}{2a_3} u_0, \tag{12}$$

or

$$\Delta G_{def,c_0=0}^{rel} = (a_1 - a_2^2/4a_3) u_0^2, \tag{13a}$$

which again is equivalent to the energy stored in a linear spring with the bilayer spring constant

$$H_B^{rel} = \left(a_1 - \frac{a_2^2}{4a_3}\right)/4. \tag{13b}$$

Equations 8, 9, 11a, b, and 13a, b provide a basis for describing the energetic consequences of inclusion-induced bilayer deformations. For either boundary condition used here, $\Delta G_{def,c_0=0}$ can be described by a linear spring model with a characteristic bilayer spring constant,

$$\Delta G_{def,c_0=0} = H_B (2u_0)^2. \tag{14}$$

The magnitude of the spring constant varies with the choice of boundary conditions (Eq. 3d or 3e) used to describe the lipid packing at the inclusion/lipid contact surface (cf. Eqs. 11b and 13b).

When $c_0 \neq 0$, the expression for ΔG_{def} (Eq. 8) contains, in addition to the quadratic terms describing $\Delta G_{def,c_0=0}$ (cf. Eq. 9), a ΔG_{MEC} term that is linear in s (Eq. 7), which has important consequences for the $\Delta G_{def}(u_0)$ relations.

REFERENCE SYSTEMS

Bilayer material constants

To evaluate the quantitative importance of the inclusion-induced deformation energy, we use experimental values of K_a and K_c for 1-stearoyl-2-oleoyl-phosphatidylcholine (SOPC), alone and with cholesterol; dioleoylphosphatidylcholine (DOPC); and glycerolmonooleate (GMO). SOPC is the reference phospholipid because its 18:0/18:1 chain composition approximates the average acyl chain composition of biological membranes (Marsh, 1990). To illustrate how the results can be extended to other systems, we use scaling relations to estimate ΔG_{def} in different systems. The scaling relations were evaluated using, first, bilayers composed of an equimolar SOPC and cholesterol mixture, which increases K_a and K_c by three- to fourfold relative to SOPC; second, bilayers composed of DOPC, in which K_c is decreased by fourfold with little change in K_a, which reduces the relevant length scale by 1/2 (Nielsen et al., 1998); and third, bilayers composed of GMO, which decreases K_a/K_c by twofold and for which there is an experimental estimate for H_B (Lundbæk and Andersen, 1999). The material constants for the four systems are listed in Table 2. There is variability among the values of material constants obtained by different investigators (cf. Needham, 1995; Nielsen et al., 1998). The values in Table 2 serve as reference points only; one can use the scaling relations to evaluate the bilayer deformation energy for any choice of material constants.

Protein models

The effects of lipid composition (bilayer mechanical characteristics) on the conformational equilibrium in membrane proteins were evaluated using, first, the transmembrane dimerization of gramicidin (gA) channels, and, second, the close↔open transition in gap junction channels. The channels are treated as rigid cylinders with the dimensions listed in Table 3.

TABLE 2 Bilayer parameters

Parameter	d_0	K_a	K_c	R_{Head}
Units	nm	pN/nm	pN · nm	nm
SOPC	3.0[c]	193[f]	90[i]	0.45[f]
SOPC:Chol (1:1)	3.3[c]	781[f]	246[i]	0.37[f]
DOPC	2.6[b]	188[e]	20[h]	0.48[g]
GMO	2.3[a]	140[d]	36[g]	0.36[g]

The SOPC reference values are denoted by asterisks in the scaling relations (Eqs. 37–39). References: a Waldbillig and Szabo (1979), Elliott et al. (1983). b Benz and Janko (1976). c Estimated values. d Chung and Caffrey (1994). e Tristram-Nagle et al. (1998). f Needham and Nunn (1990). g White (1978), Hladky and Gruen (1982). h Niggemann et al. (1995). i Evans and Rawicz (1990). Rawicz et al. (2000) have recently determined somewhat larger values for K_a and K_c in SOPC.

RESULTS

Given the structures of Eqs. 8 and 9, it is useful to start out by exploring the consequences of the biquadratic relation between $\Delta G_{def,c_0=0}$, u_0, and s (Eq. 9). The reference system will be a membrane-spanning protein with $r_0 = 3.0$ nm (corresponding to a gap junction channel) in a bilayer with properties similar to those of a SOPC bilayer with $d_0 = 3.0$ nm; the reference deformation will be a hydrophobic mismatch of 0.2 nm ($=2u_0 = d_0 - l$).

The biquadratic nature of the deformation energy

Fig. 3 shows numerical evaluations of Eq. 2 for the reference system and $c_0 = 0$. Fig. 3 *a* shows how s_{min} varies as a linear function of u_0. The compression-expansion and splay-distortion components of $\Delta G^{rel}_{def,c_0}=0$, taken together, lead to a surprising simplicity (Eq. 12). Fig. 3 *b* shows the corresponding relation between u_0 and $\Delta G^{rel}_{def,c_0}=0$, which is described by a linear spring formalism (cf. Eq. 13a). Fig. 3, *c* and *d*, shows solutions of Eq. 2 as functions of u_0 (for three fixed values of s) and s (for three fixed values of u_0). In each case $s \neq 0$ or $u_0 \neq 0$ preserves the shape of the quadratic curve but shifts the position of the minimum. The importance of the boundary conditions at r_0 is seen by comparing Fig. 3 *b* with Fig. 3, *c* and *d*.

The coefficients a_1, a_2, and a_3, which describe the system, are listed in Table 4, together with the coefficients $a_1^{CE} - a_3^{CE}$ and $a_1^{SD} - a_3^{SD}$. Given these values, $s_{min} = -0.86u_0$ (where u_0 is in nm); the two spring constants are $H_B^{con} = 88.8kT/nm^2$ (Eq. 11b) and $H_B^{rel} = 35.6kT/nm^2$ (Eq. 13b). For a given deformation, the bilayer deformation energy varies by a factor of 2.5 for the constrained as compared to the relaxed boundary condition.

The relaxed boundary condition

Combining Eqs. 7 and 9, ΔG_{def} can be expressed as a function of u_0 and s:

$$\Delta G_{def}(u_0, s) = a_1 u_0^2 + (a_2 u_0 + \alpha)s + a_3 s^2, \qquad (15)$$

TABLE 3 Inclusion parameters

Inclusion		
Reference	r_0/nm	3.0
	u_0/nm	0.1
gA channel	r_0/nm	1.0
	l/nm	2.17
Gap junction open	r_0/nm	3.0
	l_o/nm	2.985
Gap junction closed	r_0/nm	3.0
	l_c/nm	3.015

The reference r_0 is denoted by an asterisk in the scaling relations (Eq. 38).

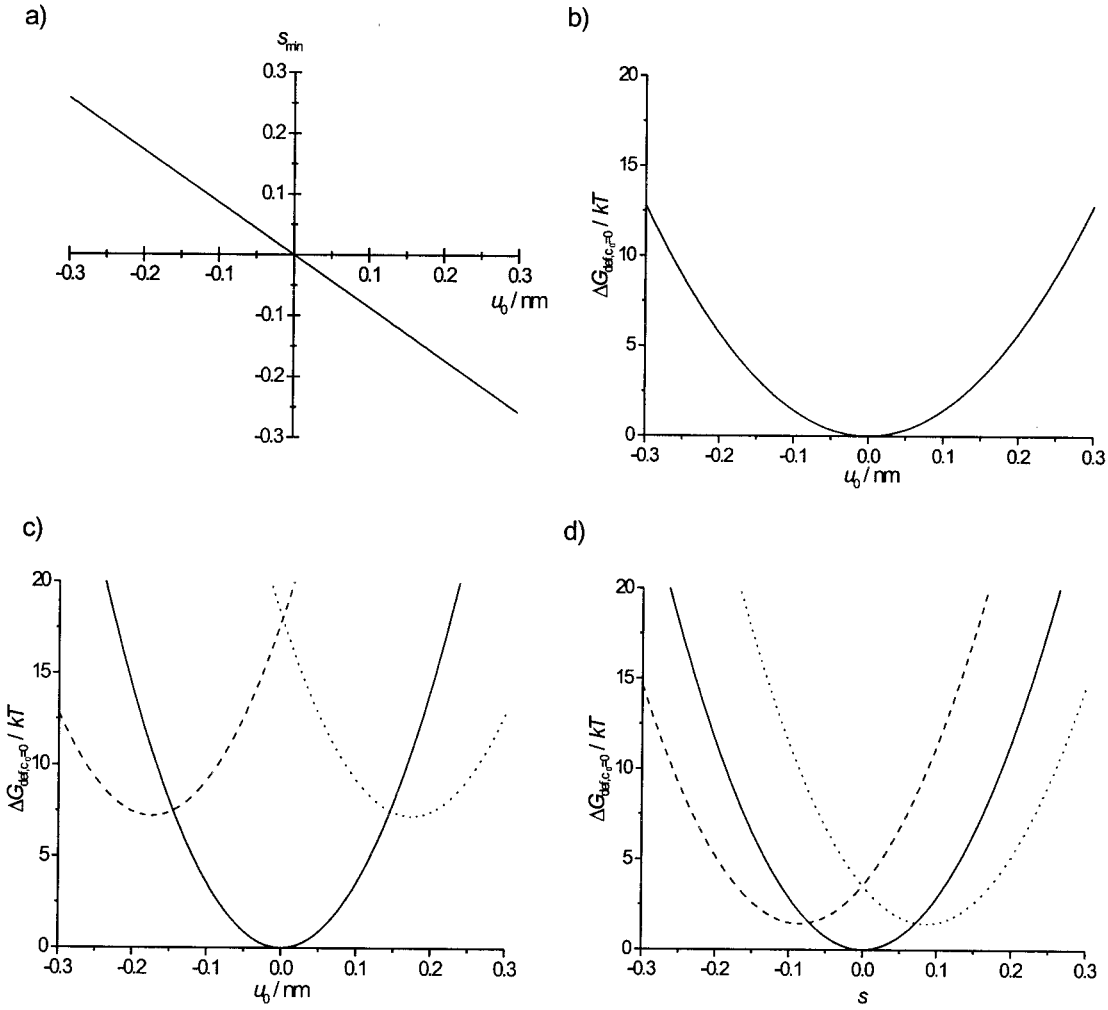

FIGURE 3 Bilayer deformations and deformation energies. (*a*) The relation between s_{min} and u_0 (Eq. 12) for a SOPC bilayer. (*b–d*) Numerical evaluation of $\Delta G_{def,c_0=0}$ (Eq. 4). The curves can be described by Eq. 9, using the $a_1^* - a_3^*$ values from Table 4. (*b*) $\Delta G_{def,c_0=0}$ for the relaxed boundary condition (Eq. 3d) as a function of the initial deformation u_0. (*c*) $\Delta G_{def,c_0=0}$ as a function of u_0 for constrained values of $s = +0.25$ (– –), $s = 0$ (—), and $s = -0.25$ (· · · · · ·). (*d*) ΔG_{def} as a function of s for constrained values of $u_0 = 0.1$ (– –), $u_0 = 0$ (—), and $u_0 = -0.1$ (· · · · · ·) nm.

where α ($=2\pi K_c r_0 c_0$) incorporates the ΔG_{MEC} contribution to ΔG_{def}. For the relaxed boundary condition and $c_0 \neq 0$, the value of s for which ΔG_{def} is a minimum is

$$s_{min} = \frac{-(a_2 u_0 + \alpha)}{2a_3}. \tag{16}$$

Substituting Eq. 16 into Eq. 15,

$$\begin{aligned}\Delta G_{def}^{rel}(u_0, c_0) &= a_1 u_0^2 - (a_2 u_0 + \alpha)\left(\frac{a_2 u_0 + \alpha}{2a_3}\right) + a_3\left(\frac{a_2 u_0 + \alpha}{2a_3}\right)^2 \\ &= -\frac{(\pi K_c r_0)^2}{a_3} c_0^2 - \frac{a_2 \pi K_c r_0}{a_3} u_0 c_0 \\ &\quad + \left(a_1 - \frac{a_2^2}{4a_3}\right) u_0^2. \end{aligned} \tag{17}$$

Fig. 4 shows ΔG_{def}^{rel} as a function of c_0 for fixed u_0, and vice versa. In either case, a u_0 (or c_0) different from zero will translate the ΔG_{def}^{rel} versus u_0 (or c_0) relation in the plane; but the basic relation, as exemplified by the spring constant, is invariant.

For any choice of u_0 or c_0, the value of ΔG_{def}^{rel} is that which minimizes the sum of the three component energies. To understand the interplay between these components, we analyze first the situation where c_0 is a free parameter (Fig. 4 *a*), then the situation where u_0 is a free parameter (Fig. 4 *b*).

TABLE 4 a_i**'s for the reference deformation in a SOPC bilayer**

i	Units for a^*	a_i^*	a_i^{CE}	a_i^{SD}
1	kT/nm^2	355	248	107
2	kT/nm	495	228	267
3	kT	288	73	215

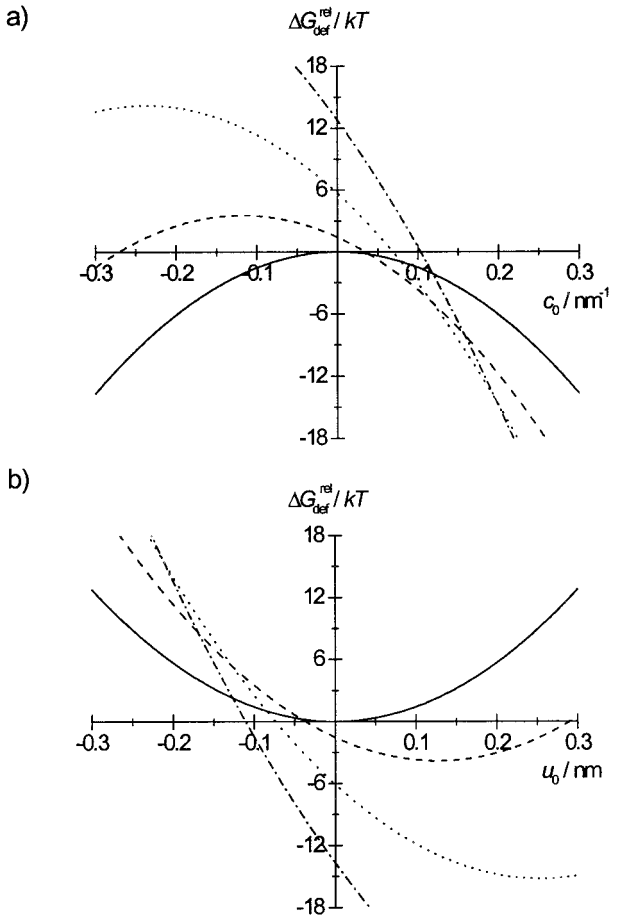

FIGURE 4 Effect of c_0 and u_0 on ΔG_{def} for the $s = s_{min}$ boundary condition. (*a*) $\Delta G_{def}^{rel}(c_0)$ for $u_0 = 0$ (—), $+0.1$ (– –), $+0.2$ (· · · · · ·), and $+0.3$ (–·–·–) nm. (*b*) $\Delta G_{def}^{rel}(u_0)$ for $c_0 = 0$ (—), $+0.1$ (– –), $+0.2$ (· · · · · ·), and $+0.3$ (–·–·–) nm^{-1}. When $u_0 < 0$, the situation is similar, with the sign of c_0 reversed (results not shown).

For a given u_0, how will the monolayer equilibrium curvature effect the deformation energy? For a fixed u_0, $\Delta G_{def}^{rel}(c_0)$ goes through a global maximum. That is, $\Delta G_{def}^{rel}(c_0)$ will have two balance points where $\Delta G_{def}^{rel}(c_0) = 0$. At these points, $\Delta G_{def,c_0}^{rel}=0$ is exactly balanced by the release of curvature frustration energy due to the monolayer bending. For a fixed $u_0 > 0$ (Fig. 4 *a*), a small positive c_0 can make $\Delta G_{def}^{rel}(c_0) = 0$; somewhat surprisingly, a large negative c_0 also can make $\Delta G_{def}^{rel}(c_0) = 0$.

For a fixed u_0, $s = 0$ at the global maximum for $\Delta G_{def}^{rel}(c_0)$ because $\partial \Delta G_{def}^{rel}/\partial \alpha = \alpha s$. Using Eq. 16, the curvature at the maximum is

$$c_0|_{max} = -[a_2/2\pi K_c r_0]u_0, \tag{18a}$$

and, combining Eqs. 17 and 18a,

$$\Delta G_{def}^{rel}(c_0)|_{max} = a_1 u_0^2, \tag{18b}$$

which is formally identical to $\Delta G_{def,c_0=0}^{con}$ (Eq. 14 with the spring constant given by Eq. 11b). The similarity is apparent, however, because $c_0|_{max}$ is a function of u_0 (Eq. 18a); but the result highlights the interactions between the bilayer material constants and the boundary conditions in determining ΔG_{def}.

For a given c_0, how will a $u_0 \neq 0$ effect ΔG_{def}? For a fixed c_0, $\Delta G_{def}^{rel}(u_0)$ will go through a global minimum (Fig. 4 *b*); when $c_0 \neq 0$, $\Delta G_{def}^{rel}(u_0)|_{min} < 0$. For $c_0 > 0$, a large positive u_0 (and a negative u_0 of more modest magnitude) can make $\Delta G_{def}^{rel}(u_0) = 0$ (Fig. 4 *b*). These balance points arise from the exact match between the release of curvature stress and $\Delta G_{def,c_0=0}^{rel}$. The situation is similar for $c_0 < 0$, but the sign of u_0 is reversed (results not shown).

The minimum of $\Delta G_{def}^{rel}(u_0)$ denotes how much energy can be released by an inclusion-induced deviation from a planar bilayer geometry. The deformation at the minimum is given by

$$u_0|_{min} = \frac{2a_2\pi K_c r_o c_0}{4a_1a_3 - a_2^2} = \left[\frac{a_2\pi K_c r_0}{8a_3 H_B^{rel}}\right]c_0 \tag{19a}$$

and

$$\Delta G_{def}^{rel}(u_0)|_{min} = -\left[\frac{a_1(\pi K_c r_o)^2}{a_1a_3 - (a_2/2)^2}\right]c_0^2. \tag{19b}$$

When $c_0 \neq 0$ the minimum for ΔG_{def} occurs at $u_0 \neq 0$. That is, a bilayer inclusion can relieve the local bilayer curvature stress, or, alternatively, the potential energy density associated with the bilayer curvature stress can drive a protein conformational change. The energy release is

$$\Delta\Delta G_{def}^{rel}(0 \rightarrow u_0|_{min}) = \Delta G_{def}^{rel}(u_0|_{min}) - \Delta G_{def}^{rel}(0)$$
$$= -\left[\frac{(a_2^2 + 8a_1a_3)(\pi K_c r_0)^2}{a_3(a_2^2 + 4a_1a_3)}\right]c_0^2. \tag{20}$$

For the reference deformation, and $c_0 = 0.1$ nm^{-1}, this energy is $-2.4kT$. It should be compared with the curvature frustration energy: $\sim 3.1kT$ if the curvature frustration energy density, $K_c c_0^2/2$, is integrated over the inclusion area, and $\sim 5.3kT$ if the energy density is integrated over the area of the inclusion plus the first annulus of lipid molecules surrounding the inclusion. Only $\sim 75\%$ of the frustration energy ($<50\%$ if we include the first lipid annulus in the appropriate area) is tapped by the $0 \rightarrow u_0|_{min}$ release.

To further understand how $c_0 \neq 0$ affects the bilayer deformation profile and energy, it is helpful to decompose $\Delta G_{def}^{rel}(c_0)$ using an expression similar to Eq. 8:

$$\Delta G_{def}^{rel}(c_0, u_0) = \Delta G_{CE}^{rel}(c_0, u_0) + \Delta G_{SD}^{rel}(c_0, u_0)$$
$$+ \Delta G_{MEC}^{rel}(c_0, u_0). \tag{21}$$

$\Delta G_{CE}^{rel}(c_0, u_0)$ and $\Delta G_{SD}^{rel}(c_0, u_0)$ are biquadratic functions of u_0 and s (Eq. 10a, b), and they can be written using Eq. 16

as

$$\Delta G_{\mathrm{CE}}^{\mathrm{rel}}(c_0, u_0) = \left(\frac{a_3^{\mathrm{CE}}(\pi K_c r_0)^2}{a_3^2}\right)c_0^2 + \left(\frac{a_3^{\mathrm{CE}}a_2}{a_3^2} - \frac{a_2^{\mathrm{CE}}}{a_3}\right)\pi K_c r_0 u_0 c_0 + \left(a_1^{\mathrm{CE}} - \frac{a_2^{\mathrm{CE}}a_2}{2a_3} + \frac{a_3^{\mathrm{CE}}a_2^2}{4a_3^2}\right)u_0^2 \quad (22a)$$

and

$$\Delta G_{\mathrm{SD}}^{\mathrm{rel}}(c_0, u_0) = \left(\frac{a_3^{\mathrm{SD}}(\pi K_c r_0)^2}{a_3^2}\right)c_0^2 + \left(\frac{a_3^{\mathrm{SD}}a_2}{a_3^2} - \frac{a_2^{\mathrm{SD}}}{a_3}\right)\pi K_c r_0 u_0 c_0 + \left(a_1^{\mathrm{SD}} - \frac{a_2^{\mathrm{SD}}a_2}{2a_3} + \frac{a_3^{\mathrm{SD}}a_2^2}{4a_3^2}\right)u_0^2. \quad (22b)$$

Similarly, $\Delta G_{\mathrm{MEC}}^{\mathrm{rel}}(c_0)$ can be written as

$$\Delta G_{\mathrm{MEC}}^{\mathrm{rel}}(c_0, u_0) = -\left(\frac{2(\pi K_c r_0)^2}{a_3}\right)c_0^2 - \left(\frac{\pi K_c r_0 a_2}{a_3}\right)u_0 c_0. \quad (23)$$

Fig. 5 shows $\Delta G_{\mathrm{CE}}^{\mathrm{rel}}(c_0)$, $\Delta G_{\mathrm{SD}}^{\mathrm{rel}}(c_0)$, $\Delta G_{\mathrm{MEC}}^{\mathrm{rel}}(c_0)$, and $\Delta G_{\mathrm{def}}^{\mathrm{rel}}(c_0)$ for the reference deformation. $\Delta G_{\mathrm{CE}}^{\mathrm{rel}}(c_0)$ and $\Delta G_{\mathrm{SD}}^{\mathrm{rel}}(c_0)$ are always positive: $\Delta G_{\mathrm{SD}}^{\mathrm{rel}}(c_0)$ has a minimum for $c_0 < 0$ and $\Delta G_{\mathrm{CE}}^{\mathrm{rel}}(c_0)$ has a minimum for $c_0 > 0$. $\Delta G_{\mathrm{MEC}}^{\mathrm{rel}}(c_0)$ has a maximum (> 0) and becomes negative for large negative and positive values of c_0. $\Delta G_{\mathrm{MEC}}^{\mathrm{rel}}(c_0) = 0$ when either $c_0 = 0$ or $s = 0$ (cf. Eq. 7).

The maximum value of $\Delta G_{\mathrm{def}}^{\mathrm{rel}}(c_0)$ is > 0, and it is important to understand the behavior at the two balance points, where $\Delta G_{\mathrm{def}}^{\mathrm{rel}}(c_0) = 0$, where the system has "tapped" the potential energy stored in the curvature frustration energy. The balance points occur when the discriminant of Eq. 15 is zero:

$$\sqrt{(a_1u_0 + \alpha)^2 - 4a_3a_1u_0^2} = 0, \quad (24)$$

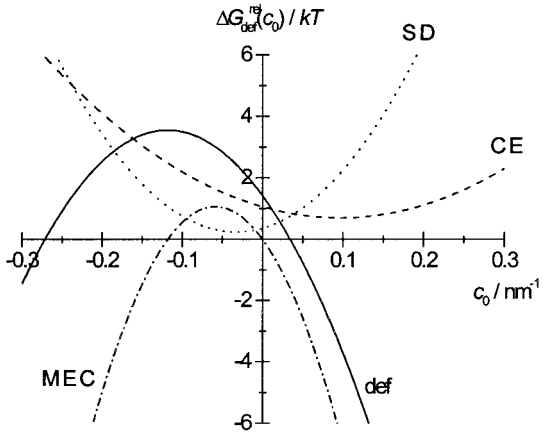

FIGURE 5 Effect of c_0 on $\Delta G_{\mathrm{def}}^{\mathrm{rel}}$ for a fixed u_0 (=0.1 nm): $\Delta G_{\mathrm{def}}^{\mathrm{rel}}(c_0)$ (—) and its components. – – – –, $\Delta G_{\mathrm{CE}}^{\mathrm{rel}}(c_0)$; · · · · · ·, $\Delta G_{\mathrm{SD}}^{\mathrm{rel}}(c_0)$; —·—, $\Delta G_{\mathrm{MEC}}^{\mathrm{rel}}(c_0)$.

which is the case when

$$\alpha = 2\pi K_c c_0 r_0 = -a_2u_0 \pm 2u_0\sqrt{a_3a_1}. \quad (25)$$

Equation 25 can be solved for u_0 (at a fixed c_0) or c_0 (at a fixed u_0):

$$c_0 = \frac{-a_2u_0 \pm 2u_0\sqrt{a_3a_1}}{2\pi K_c r_0} \quad (26a)$$

$$u_0 = \frac{-2\pi K_c c_0 r_0}{a_2 \pm 2\sqrt{a_3a_1}}. \quad (26b)$$

Combining Eqs. 15 and 25, the s values that satisfy the $\Delta G_{\mathrm{def}}^{\mathrm{rel}}(c_0) = 0$ condition are

$$s = \mp u_0\sqrt{\frac{a_1}{a_3}}. \quad (27)$$

To understand the two solutions, consider a hypothetical situation where c_0 is varied by pharmacological manipulations, with no change in the other material constants. When $c_0 = 0$, there will be a finite bilayer deformation energy when $u_0 \neq 0$. For a fixed u_0, it is possible to change c_0 such that the local relief of curvature stress around the inclusion will balance exactly the deformation energy at $c_0 = 0$. This balance can occur for two different values of c_0. The origin of the two balance points is seen in Fig. 6 *a*, which shows how the c_0-dependent translation of the $\Delta G_{\mathrm{def},c_0}^{\mathrm{rel}}=0(s)$ curve gives rise to two different solutions for $\Delta G_{\mathrm{MEC}}^{\mathrm{rel}}(c_0)$, where c_0 is determined by Eq. 26a. The solution for $c_0 > 0$ makes intuitive sense because $u_0 > 0$. A positive curvature will facilitate the dimpling needed to satisfy the demand for hydrophobic matching. The counterintuitive solution for $c_0 < 0$ arises because it is the sum of the CE, SD, and MEC contributions to $\Delta G_{\mathrm{def}}^{\mathrm{rel}}$ that is minimized. The bilayer can relieve its curvature stress by assuming another positive value of s_{min}, which leads to a different profile for the component energies. Fig. 6 *b* shows the two u_0 versus c_0 relations (Eq. 26b), and Fig. 6, *c* and *d*, shows the monolayer deformation profiles for the two solutions. For either solution, the profile is nonmonotonic. As expected, the nonmonotonic shape is most pronounced for $c_0 < 0$ (Fig. 6 *d*).

To understand the relationship between $\Delta G_{\mathrm{def}}^{\mathrm{rel}}$ and u_0 (for a fixed $c_0 \neq 0$), we examine the underlying energy components (Fig. 7). $\Delta G_{\mathrm{CE}}^{\mathrm{rel}}(u_0)$ and $\Delta G_{\mathrm{SD}}^{\mathrm{rel}}(u_0)$ (Eq. 22a, b) are always positive (Fig. 7 *a*); $\Delta G_{\mathrm{SD}}^{\mathrm{rel}}(u_0)$ has a minimum for $u_0 < 0$, whereas the minimum for $\Delta G_{\mathrm{CE}}^{\mathrm{rel}}(u_0)$ occurs for $u_0 > 0$ (for $c_0 > 0$). $\Delta G_{\mathrm{MEC}}^{\mathrm{rel}}(u_0)$ is a linear function of u_0 (Eq. 28) and becomes negative when $u_0 > -2\pi K_c r_0 c_0/a_2$. The magnitude of $\Delta G_{\mathrm{MEC}}^{\mathrm{rel}}(u_0)$ ensures that the global minimum for $\Delta G_{\mathrm{def}}^{\mathrm{rel}}(u_0)$ will be negative (Eq. 19b). The $\Delta G_{\mathrm{MEC}}^{\mathrm{rel}}(u_0)$ contribution will promote a nonplanar profile of the bilayer-solution interface in the vicinity of the inclusion, which means that the curvature stress (due to $c_0 \neq 0$) can "drive"

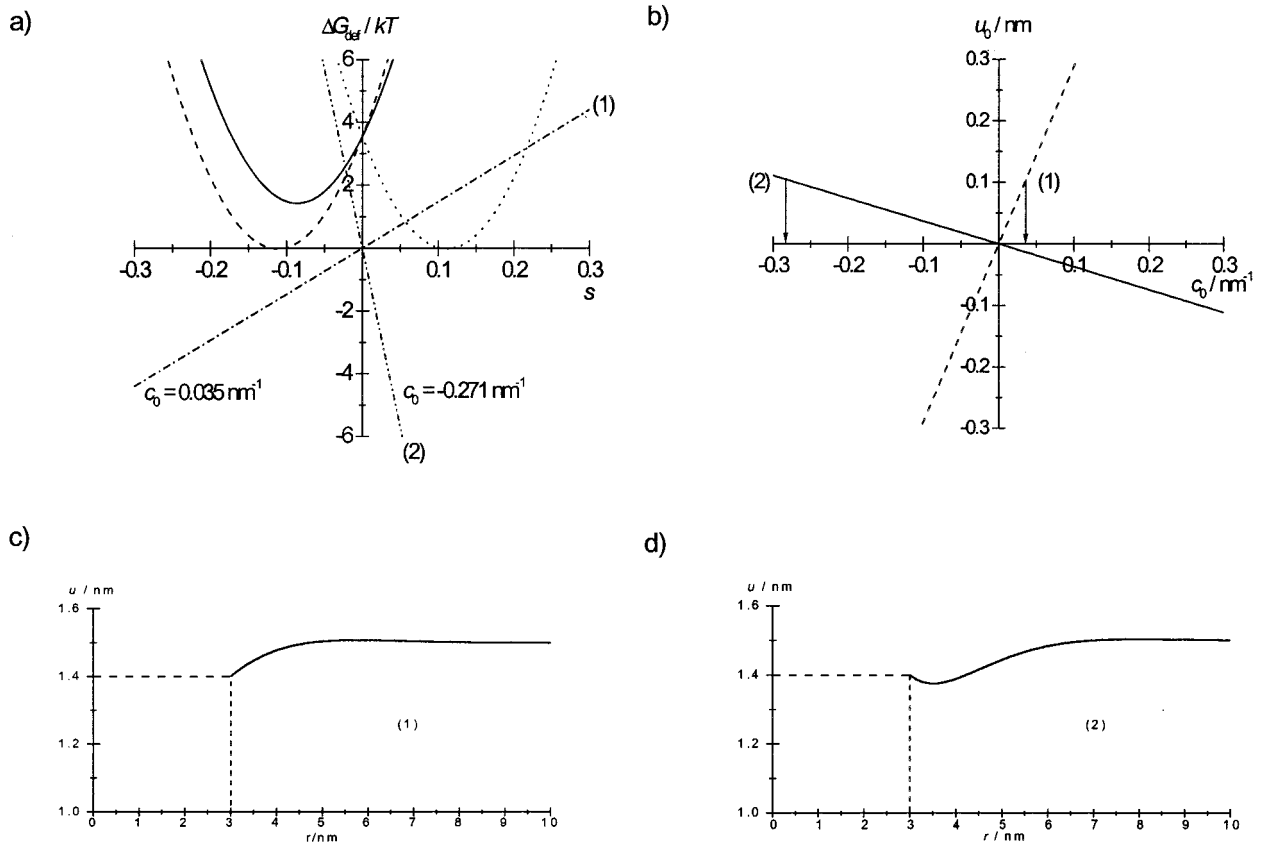

FIGURE 6 Effect of c_0 on ΔG_{def} and the deformation profile. (*a*) Effect of monolayer curvature on $\Delta G_{\text{def}}(s)$ for a fixed u_0 (=0.1 nm). —, $\Delta G_{\text{def},c_0=0}$. – – and · · · · · · are the $\Delta G_{\text{def}}(s)$ relations that satisfy the $\Delta G^{\text{rel}}_{\text{def}}(c_0) = 0$ condition (where c_0 is determined by Eq. 26a). The corresponding ΔG_{MEC} contributions are shown as dotted dashed lines (labeled (1) and (2)). (*b*) The two solutions for u_0 as function of c_0 (Eq. 26b). The two $\Delta G_{\text{def}}(s) = 0$ solutions from *a* are labeled (1) and (2). (*c*) The monolayer deformation profile for $c_0 = 0.035\ \text{nm}^{-1}$ and $s = -0.111$ (solution (1)). (*d*) The monolayer deformation profile for $c_0 = -0.271\ \text{nm}^{-1}$ and $s = 0.111$ (solution (2)).

a membrane protein conformational change. The monolayer deformation profile at the minimum is shown in Fig. 7 *b*; again the profile is nonmonotonic.

The constrained boundary condition

For $s = 0$ the ΔG_{MEC} contribution to $\Delta G^{\text{con}}_{\text{def}}$ is zero (Eq. 7). The combination $c_0 \neq 0$ and $s = 0$ is unlikely, however, because a close alignment of noncylindrical lipid molecules around the inclusion will tend to force s to be different from zero. Geometric arguments lead to Eq. 3f as a limiting boundary condition, in which case,

$$\begin{aligned}\Delta G^{\text{con}}_{\text{def}}(c_0, u_0) &= a_1 u_0^2 + (a_2 u_0 + \alpha) R_{\text{Head}} c_0 + a_3 (R_{\text{Head}} c_0)^2 \\ &= (2\pi K_c r_0 R_{\text{Head}} + a_3 R_{\text{Head}}^2) c_0^2 + R_{\text{Head}} a_2 u_0 c_0 \\ &\quad + a_1 u_0^2. \end{aligned} \tag{28}$$

Fig. 8 shows $\Delta G^{\text{con}}_{\text{def}}$ as a function of c_0 for fixed u_0, and vice versa. A c_0 (or u_0) different from zero will translate the $\Delta G^{\text{con}}_{\text{def}}$ versus u_0 (or c_0) relation in the plane (cf. Eq. 28); but, as was the case for the relaxed boundary condition, the basic relation is invariant. First, we describe the situation where c_0 is a free parameter (Fig. 8 *a*); then we describe the situation where u_0 is a free parameter (Fig. 8 *b*).

For fixed u_0, Eq. 28 has a global minimum at

$$c_0|_{\text{min}} = -\left[\frac{a_2}{2(2\pi K_c r_0 + a_3 R_{\text{Head}})}\right] u_0, \tag{29a}$$

where

$$\Delta G^{\text{con}}_{\text{def}}(c_0, u_0)|_{\text{min}} = \left[a_1 - \frac{a_2^2}{4((2\pi K_c r_0 / R_{\text{Head}}) + a_3)}\right] u_0^2. \tag{29b}$$

When compared to the relaxed boundary condition (Eq. 17), the effects of a given $c_0 \neq 0$ are qualitatively different for the constrained boundary condition (cf. Figs. 4 *a* and 8 *a*). Importantly, the shapes of the $\Delta G^{\text{con}}_{\text{def}}(c_0)$ relations are quite different for the two boundary conditions.

The importance of the lipid packing constraints can be illustrated by comparing the spring constant in Eq. 29b with the ones in Eqs. 11a and 13a. Because $2\pi K_c r_0 / R_{\text{Head}} > 0$, the spring constant in Eq. 29b is larger than $a_1 - a_2^2/4a_3$ but

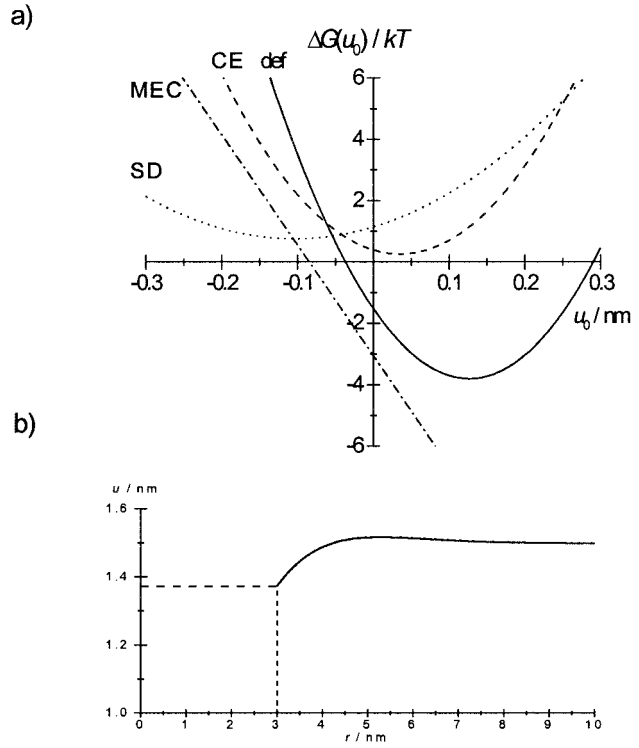

FIGURE 7 Effect of u_0 on $\Delta G_{\mathrm{def}}^{\mathrm{rel}}$ and the deformation profile for a fixed c_0 (=0.1 nm^{-1}). (*a*) $\Delta G_{\mathrm{def}}^{\mathrm{rel}}(u_0)$ (—), $\Delta G_{\mathrm{CE}}^{\mathrm{rel}}(u_0)$ (– –), $\Delta G_{\mathrm{SD}}^{\mathrm{rel}}(u_0)$ (· · · · · ·), and $\Delta G_{\mathrm{MEC}}^{\mathrm{rel}}(u_0)$ (–·–·–). The minimum for $\Delta G_{\mathrm{def}}^{\mathrm{rel}}(u_0)$ is $-3.81kT$ (u_0 = 0.127 nm); the corresponding $s_{\mathrm{min}} = -0.182$. (*b*) The monolayer deformation profile for these values of u_0 and s_{min}.

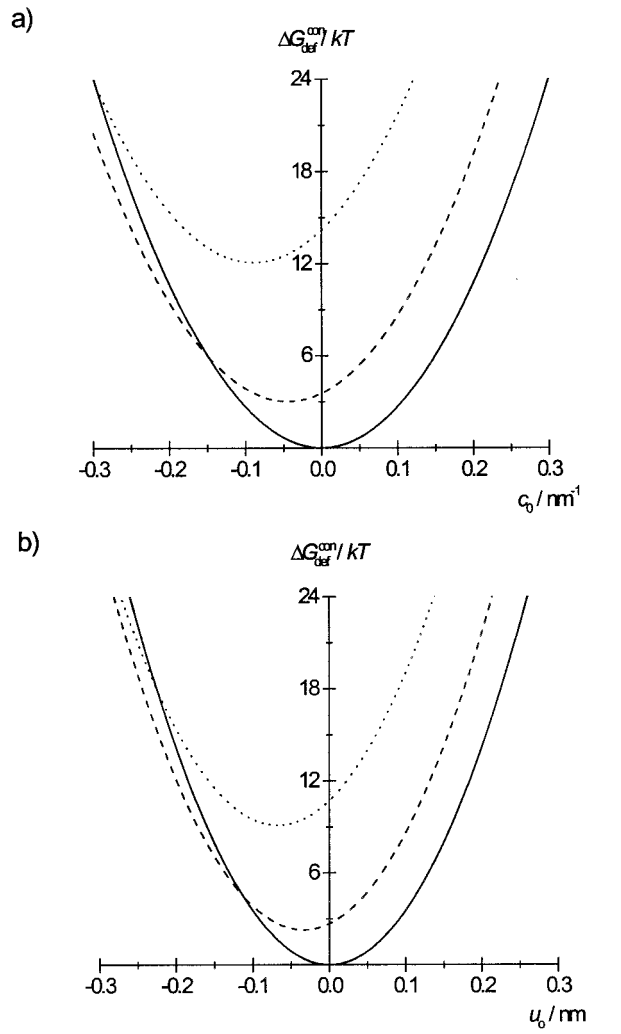

FIGURE 8 Effect of curvature on $\Delta G_{\mathrm{def}}^{\mathrm{con}}$ in the reference system. (*a*) $\Delta G_{\mathrm{def}}^{\mathrm{con}}(c_0)$ for $u_0 = 0$ (—), 0.1 (– –), and 0.2 (· · · · · ·) nm. (*b*) $\Delta G_{\mathrm{def}}^{\mathrm{con}}(u_0)$ for $c_0 = 0$ (—), 0.1 (– –), and 0.2 (· · · · · ·) nm^{-1}.

less than a_1. Using the standard parameter set, $\Delta G_{\mathrm{def}}^{\mathrm{con}}(c_0, 0.1)|_{\mathrm{min}} = 3.0kT$ (u_0 in nm), which should be compared to $\Delta G_{\mathrm{def},c_0}^{\mathrm{rel}}=0 = 1.4kT$ and $\Delta G_{\mathrm{def},c_0}^{\mathrm{con}}=0 = 3.6kT$. The curvature is allowed to vary, such that the system relaxes toward its minimum energy configuration, but the deformation energy is twofold higher than $\Delta G_{\mathrm{def},c_0}^{\mathrm{rel}}=0$ and close to $\Delta G_{\mathrm{def},c_0}^{\mathrm{con}}=0$. The constraints imposed by the local lipid packing around the inclusion have important consequences for the bilayer deformation energy.

For the constrained boundary condition, how will a $c_0 \neq 0$ affect the inclusion-induced deformation energy? The deformation energy is always positive (Fig. 8 *b*), and, for fixed c_0, $\Delta G_{\mathrm{def}}^{\mathrm{con}}(c_0, u_0)$ has a global minimum at

$$u_0|_{\mathrm{min}} = -\left[\frac{R_{\mathrm{Head}}a_2}{2a_1}\right]c_0, \tag{30a}$$

in which case

$$\Delta G_{\mathrm{def}}^{\mathrm{con}}(u_0|_{\mathrm{min}}) = \left[2\pi K_{\mathrm{c}} r_0 R_{\mathrm{Head}} + \frac{R_{\mathrm{Head}}^2(4a_1a_3 - a_2^2)}{4a_1}\right]c_0^2. \tag{30b}$$

That is, there is a linear relation between this minimum bilayer deformation and c_0, and the minimum deformation energy varies as a quadratic function of c_0; but $\Delta G_{\mathrm{def}}^{\mathrm{con}}(u_0)|_{\mathrm{min}} \geq 0$. The energy that is released when u_0 changes from 0 to $u_0|_{\mathrm{min}}$ can "drive" a protein conformational change. This energy is

$$\Delta\Delta G_{\mathrm{def}}^{\mathrm{con}}(0 \rightarrow u_0|_{\mathrm{min}}) = \Delta G_{\mathrm{def}}^{\mathrm{con}}(u_0|_{\mathrm{min}}) - \Delta G_{\mathrm{def}}^{\mathrm{con}}(0) = \frac{-R_{\mathrm{Head}}^2 a_2^2 c_0^2}{4a_1} = -H_{\mathrm{B}}^{\mathrm{con}}(2u_0|_{\mathrm{min}})^2, \tag{31}$$

an expression that should be compared to Eq. 11a, b and Eq. 20. (Using Eq. 3f, an inclusion will induce a nonplanar bilayer deformation when $c_0 \neq 0$, even though $u_0 = 0$, and $\Delta G_{\mathrm{def}}^{\mathrm{con}}(c_0, 0)$ denotes the curvature stress induced by the finite c_0 over the bilayer that is perturbed by the inclusion.) For the reference deformation, $\Delta\Delta G_{\mathrm{def}}^{\mathrm{con}}(0 \rightarrow u_0|_{\mathrm{min}}) = -0.39kT$; only 13% (7% if we include the first lipid annu-

lus) of the frustration energy ($3.1kT$) is tapped by the $0 \rightarrow u_0|_{\min}$ release. This very modest release of the curvature frustration energy results from the c_0-dependent constraints on s (Eq. 3f), which are in a direction opposite that of the one that in a straightforward manner would release the curvature-induced stress.

Again, it is useful to decompose $\Delta G_{\mathrm{def}}^{\mathrm{con}}$ into the component energies:

$$\Delta G_{\mathrm{def}}^{\mathrm{con}}(c_0, u_0) = \Delta G_{\mathrm{CE}}^{\mathrm{con}}(c_0, u_0) + \Delta G_{\mathrm{SD}}^{\mathrm{con}}(c_0, u_0) + \Delta G_{\mathrm{MEC}}^{\mathrm{con}}(c_0, u_0), \quad (32)$$

where

$$\Delta G_{\mathrm{CE}}^{\mathrm{con}}(c_0, u_0) = a_1^{\mathrm{CE}} u_0^2 + a_2^{\mathrm{CE}} u_0 R_{\mathrm{Head}} c_0 + a_3^{\mathrm{CE}} (R_{\mathrm{Head}} c_0)^2 \quad (33a)$$

$$\Delta G_{\mathrm{SD}}^{\mathrm{con}}(c_0, u_0) = a_1^{\mathrm{SD}} u_0^2 + a_2^{\mathrm{SD}} u_0 R_{\mathrm{Head}} c_0 + a_3^{\mathrm{SD}} (R_{\mathrm{Head}} c_0)^2 \quad (33b)$$

and

$$\Delta G_{\mathrm{MEC}}^{\mathrm{con}}(c_0, u_0) = 2\pi K_{\mathrm{c}} r_0 R_{\mathrm{Head}} c_0^2. \quad (34)$$

Fig. 9 *a* shows results with c_0 as a free parameter (u_0 = 0.1 nm). $\Delta G_{\mathrm{CE}}^{\mathrm{con}}(c_0)$, $\Delta G_{\mathrm{SD}}^{\mathrm{con}}(c_0)$, and $\Delta G_{\mathrm{MEC}}^{\mathrm{con}}(c_0)$, as well as $\Delta G_{\mathrm{def}}^{\mathrm{con}}(c_0)$, are all ≥ 0. $\Delta G_{\mathrm{CE}}^{\mathrm{con}}(c_0)$ and $\Delta G_{\mathrm{SD}}^{\mathrm{con}}(c_0)$ are positive definite with global minima for $c_0 < 0$ (because $u_0 > 0$). The global minimum for $\Delta G_{\mathrm{MEC}}^{\mathrm{con}}(c_0)$ is zero and occurs at $c_0 = 0$. $\Delta G_{\mathrm{def}}^{\mathrm{con}}(c_0)$ is always positive with a global minimum at $c_0 < 0$ (when $u_0 > 0$). The curvature contribution to $\Delta G_{\mathrm{def}}^{\mathrm{con}}(c_0)$ will promote a nonplanar bilayer profile in the vicinity of the inclusion, which means that the curvature stress can "drive" a protein conformational change even though $\Delta G_{\mathrm{MEC}}^{\mathrm{con}}(u_0)|_{\min} > 0$; but the inclusion can "tap" only a small fraction of the energy.

Fig. 9 *b* shows the corresponding results with u_0 as a free parameter ($c_0 = 0.1\ \mathrm{nm}^{-1}$). The situation is similar to that in Fig. 9 *a*, except that $\Delta G_{\mathrm{MEC}}^{\mathrm{con}}(u_0)$ is constant. $\Delta G_{\mathrm{def}}^{\mathrm{con}}(u_0)$ is always positive, and the global minimum occurs for $u_0 < 0$ (when $c_0 > 0$).

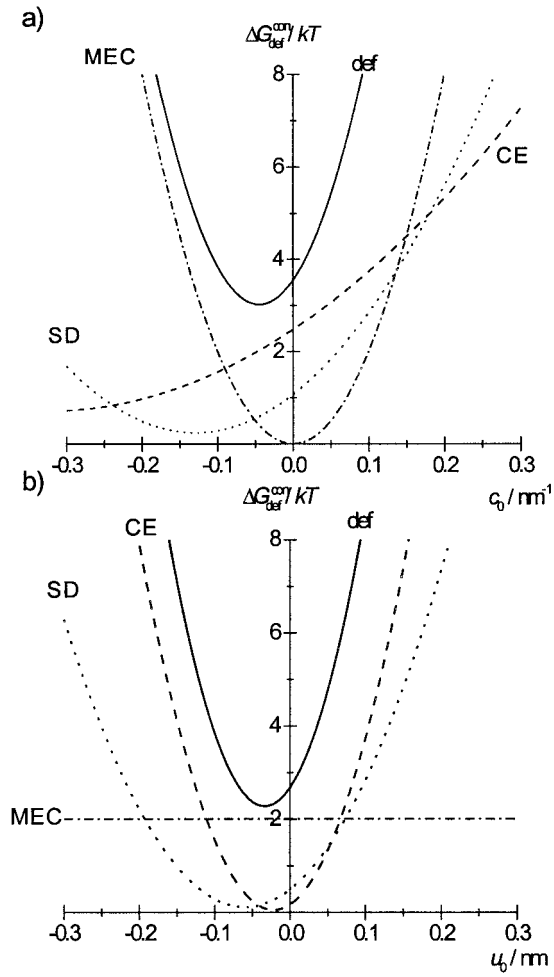

FIGURE 9 Effects of c_0 and u_0 on $\Delta G_{\mathrm{def}}^{\mathrm{con}}$. (*a*) $\Delta G_{\mathrm{def}}^{\mathrm{con}}(c_0)$ for fixed u_0 (=0.1 nm) (—) together with its components: $\Delta G_{\mathrm{CE}}^{\mathrm{con}}(c_0)$ (– –), $\Delta G_{\mathrm{SD}}^{\mathrm{con}}(c_0)$ (· · · · · ·), and $\Delta G_{\mathrm{MEC}}^{\mathrm{con}}(c_0)$ (–·–·–). (*b*) $\Delta G_{\mathrm{def}}^{\mathrm{con}}(u_0)$ for fixed c_0 (=0.1 nm^{-1}) (—), together with its components: $\Delta G_{\mathrm{CE}}^{\mathrm{con}}(u_0)$ (– –), $\Delta G_{\mathrm{SD}}^{\mathrm{con}}(u_0)$ (· · · · · ·), and $\Delta G_{\mathrm{MEC}}^{\mathrm{con}}(u_0)$ (–·–·–).

Scaling relations

We have illustrated the energetic and conformational consequences of a nonzero monolayer equilibrium curvature on a "standard inclusion" in a SOPC bilayer. But the bilayer deformation energy varies as a function of the bilayer mechanical properties as well as the inclusion dimensions. It therefore is important to be able to estimate the bilayer deformation energy for other systems. To this end, we examine how the results obtained for our reference system scale as a function of bilayer mechanical moduli and inclusion dimensions (cf. the scaling relations in Nielsen et al., 1998). Because the energy components are interdependent, it also is important to know how this interdependence affects the scaling relations. First, we investigate the interdependence; then we deduce the scaling relations.

Fig. 10 shows $\Delta G_{\mathrm{def},c_0=0}^{\mathrm{con}}$ as function of K_{a} and K_{c}. Because $\Delta G_{\mathrm{def},c_0=0} = H_{\mathrm{B}} u_0^2$, the scaling properties can be expressed as

$$H_{\mathrm{B}} \sim H_{\mathrm{B}}^{*} \left(\frac{K_{\mathrm{a}}}{K_{\mathrm{a}}^{*}} \right)^{n_{\mathrm{a}}} \quad (35)$$

and

$$H_{\mathrm{B}} \sim H_{\mathrm{B}}^{*} \left(\frac{K_{\mathrm{c}}}{K_{\mathrm{c}}^{*}} \right)^{n_{\mathrm{c}}}, \quad (36)$$

where the superscript * denotes the chosen reference parameters. In Eqs. 35 and 36, n_{a} is determined by varying K_{a} for fixed K_{c} (Fig. 10 *a*) and vice versa for n_{c} (results not shown). Similar results were obtained for $\Delta G_{\mathrm{def},c_0=0}^{\mathrm{rel}}$ (results

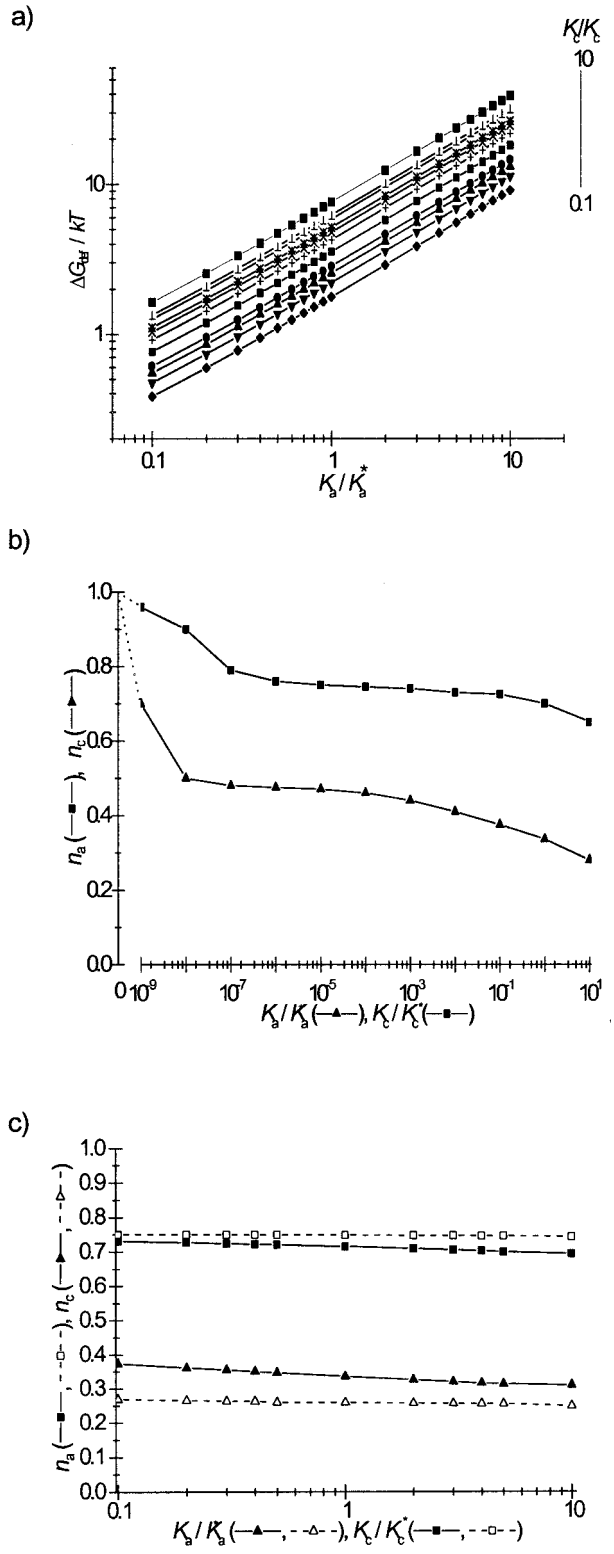

FIGURE 10 Scaling relations. (*a*) The relation between $\Delta G^{con}_{def,c_0}=0$ and K_a/K_a^* for K_c/K_c^* values ranging between 0.1 and 10, which allows for determination of n_a (the corresponding figure for n_c is similar; not shown). Each point denotes an evaluation of Eq. 4 for the reference system (u_0 = 0.1 nm) and the indicated modulus. The lines are nonlinear fits to $\bar{a}(K_a/K_a^*)^{n_a} + \hat{a}$ with mean value $n_a = 0.721$ ($\chi^2 < 0.01$). (*b*) n_a versus K_c/K_c^* for $K_a = K_a^*$ (■) and n_c versus K_a/K_a^* for $K_c = K_c^*$ (▲). Each point corresponds to an n value as determined in *a*. (*c*) n_a (■) and n_c (▲) for different ratios of K_a/K_a^* or K_c/K_c^* for $s = 0$ (—) and $s = s_{min}$ (——). Lines denote fits to a power relation $y = ax^b + c$, where $-0.04 \le b \le -0.002$. For the unity ratios: $n_a(s = 0) = 0.714$, $n_a(s = s_{min}) = 0.748$, $n_c(s = 0) = 0.342$, and $n_c(s = s_{min}) = 0.260$.

not shown). $\Delta G_{def,c_0=0}$ is proportional to H_B, and a twofold increase in H_B increases $\Delta G_{def,c_0=0}$ by twofold. Similarly, a twofold increase in both K_a and K_c causes a twofold increase in $\Delta G_{def,c_0=0}$ (and H_B). One therefore would expect that $n_a + n_c = 1$. Indeed, $n_a + n_c \approx 1$ when both $K_a/K_a^* \gg 1$ and $K_c/K_c^* \gg 1$. But when either $K_a/K_a^* \ll 1$ or $K_c/K_c^* \ll 1$, $n_a + n_c \neq 1$, a result that arises because, when $K_c \to 0$ (and therefore $\Delta G_{SD} \to 0$), ΔG_{CE} will be finite as long as $K_a > 0$, and vice versa. In the limit when $K_c = 0$ (and $K_a > 0$), $n_a = 1$; correspondingly, when $K_a = 0$ (and $K_c > 0$), $n_c = 1$ (Fig. 10 *b*). Because ΔG_{SD} and ΔG_{CE} are functions of both moduli, the energy terms are interdependent, which is evident in Fig. 10 *c*, which explains why $n_a + n_c \neq 1$. (Actually, $n_a + n_c$ will always be >1). For $s = s_{min}$, n_a varies by less than 5% for K_c/K_c^* ranging between 0.1 and 10, and n_c varies by <5% for K_a/K_a^* ranging between 0.1 and 10. For $s = 0$, the corresponding variations are less than 15%.

The situation is more complex when $c_0 \neq 0$ because the simple spring model is no longer sufficient to describe the system. In this case scaling relations for the a_i coefficients (Eq. 9) provide a more useful framework for evaluating ΔG_{def}. Fig. 11 shows a_1, a_2, and a_3 as functions of K_a, K_c, r_0, and d_0. The $a_i(K_x)$ relations can be described by expressions of the form (*solid lines* in Fig. 11)

$$a_i = \bar{a}_i\left(\frac{K_x}{K_x^*}\right)^{n_{x,i}} + \hat{a}_i, \tag{37}$$

where the subscript $x = a, c$; $i = 1, 2, 3$; and $a_i^* = \bar{a}_i + \hat{a}_i$. Table 5 summarizes results for $n_{x,i}$, $\bar{a}_i$, and $\hat{a}_i$ obtained by least-squares fitting to the results shown in Fig. 11, *a* and *b*. Except for $\hat{a}_i$ when $K = K_a$, $\hat{a}_i/\bar{a}_i \ll 1$. The $a_i(d_0)$ and $a_i(r_0)$ relations (Fig. 11, *c* and *d*) can be described by similar expressions:

$$a_i = \bar{a}_i\left(\frac{d_0}{d_0^*}\right)^{n_{d,i}} + \hat{a}_i \tag{38}$$

and

$$a_i = \bar{a}_i\left(\frac{r_0}{r_0^*}\right)^{n_{r,i}} + \hat{a}_i, \tag{39}$$

where $a_i^* = \bar{a}_i + \hat{a}_i$. The estimates for n_i, $\bar{a}_i$, $\hat{a}_i$, and n_i also are listed in Table 5. Similar scaling relations can be derived for the CE and SD coefficients a_1^{CE}, a_2^{CE}, and a_3^{CE} and a_1^{SD}, a_2^{SD}, and a_3^{SD}; the results are summarized in Tables 6 and 7.

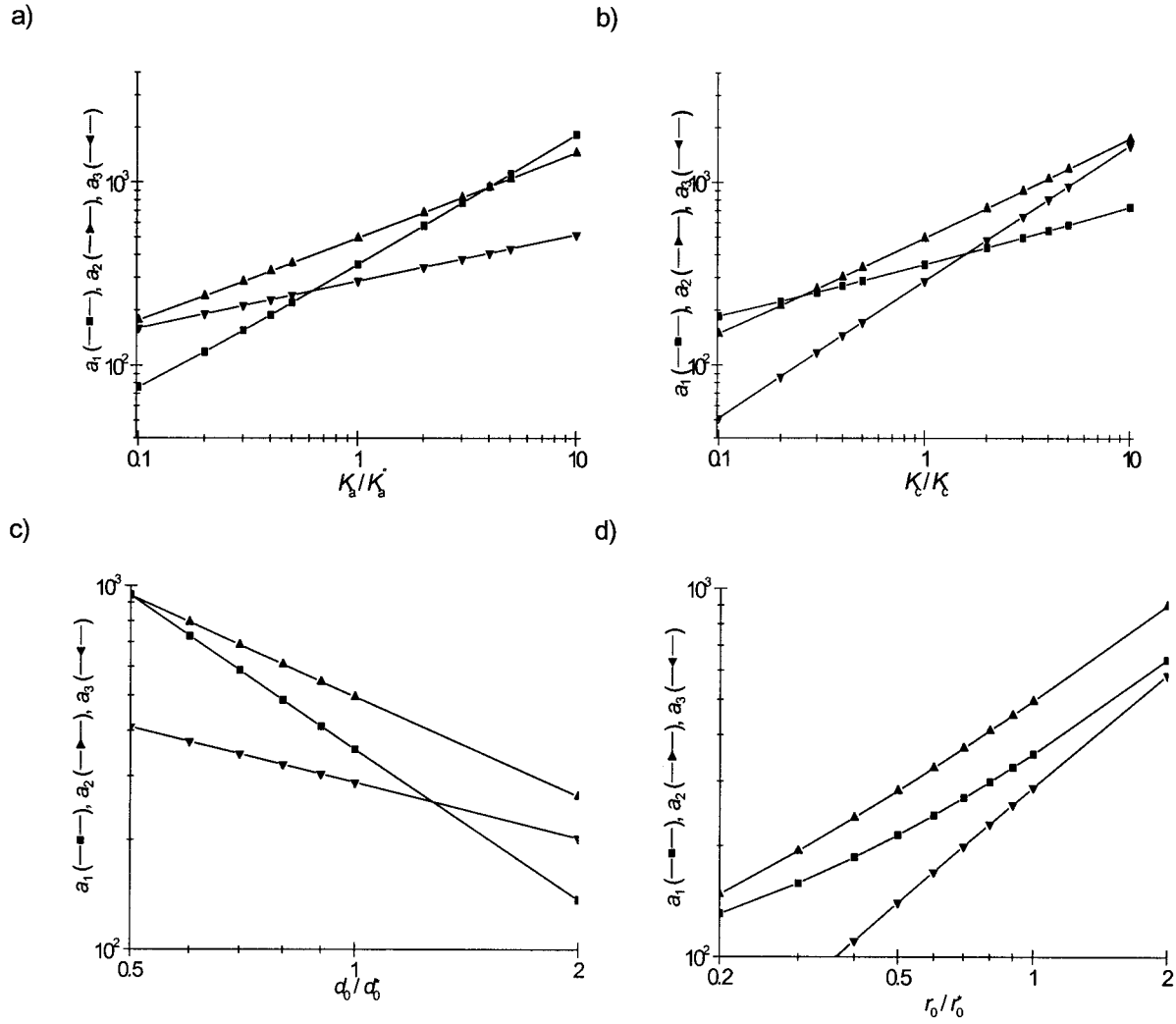

FIGURE 11 Scaling relations for a_1, a_2, a_3. (*a*) Results for K_a/K_a^*. (*b*) Results for K_c/K_c^*. (*c*) Results for d_0/d_0^*. (*d*) Results for r_0/r_0^*. The points denote evaluations of Eq. 9 based on evaluations of Eq. 4 for the reference system ($u_0 = 0.1$ nm), with the indicated modulus varied and s varying in increments of 0.01 from -1 to 1. The lines are nonlinear fits to Eqs. 37–39 ($\chi^2 < 0.01$). The parameters are listed in Table 5.

To use the scaling relations, consider an inclusion with the dimensions of a gA channel embedded in a GMO bilayer. The gA system is important because it provides a direct link between the theoretical predictions and experimental reality (Lundbæk and Andersen, 1999; Andersen et al., 1999). Using Table 5 (and Tables 2 and 3), $a_1 = 124.7kT/\text{nm}^2$; $a_2 = 126.3kT/\text{nm}$; and $a_3 = 45.8kT$. The spring constant estimates for the GMO + gA system are $H_B^{con} = 31.2kT/\text{nm}^2$ and $H_B^{rel} = 9.4kT/\text{nm}^2$ (and $s_{min} = -0.138$), which should be compared with direct evaluations based on Eq. 2: $H_B^{con} = 30.3kT/\text{nm}^2$; $H_B^{rel} = 10.1kT/\text{nm}^2$; and $s_{min} = -0.122$. The scaling relations are accurate to ~10%. The spring constant estimates also should be compared with the experimentally determined spring constant $H_B = 28.3kT/\text{nm}^2$ (Lundbæk and Andersen, 1999), which suggests that the appropriate boundary condition is $s = 0$.

DISCUSSION

The lipid bilayer components of cellular membranes are permeability barriers. But phospholipid extracts from bio-

TABLE 5 Parameterization of $\Delta G_{def,c_0=0}$

i	$\bar{a}_{a,i}$	$\hat{a}_{a,i}$	$n_{a,i}$	$\bar{a}_{c,i}$	$\hat{a}_{c,i}$	$n_{c,i}$	$\bar{a}_{d,i}$	$\hat{a}_{d,i}$	$n_{d,i}$	$\bar{a}_{r,i}$	$\hat{a}_{r,i}$	$n_{r,i}$
1	344.5	10.5	0.721	308.5	46.5	0.348	347.0	8.0	−1.430	278.0	77.0	1.023
2	476.2	18.5	0.479	479.0	16.0	0.558	478.6	16.4	−0.951	448.6	46.4	0.926
3	294.2	−6.2	0.249	290.2	−1.5	0.742	294.6	−6.6	−0.498	297.4	−9.4	0.992

TABLE 6 Parameterization of $\Delta G_{CE,c_0=0}$

i	$\bar{a}_{a,i}$	$\hat{a}_{a,i}$	$n_{a,i}$	$\bar{a}_{c,i}$	$\hat{a}_{c,i}$	$n_{c,i}$	$\bar{a}_{d,i}$	$\hat{a}_{d,i}$	$n_{d,i}$	$\bar{a}_{r,i}$	$\hat{a}_{r,i}$	$n_{r,i}$
1	242.9	5.1	0.730	220.2	27.8	0.323	244.0	4.0	−1.453	211.3	36.7	1.015
2	221.5	6.5	0.488	221.1	6.9	0.542	222.1	5.9	−0.972	209.3	18.7	0.978
3	72.7	0.3	0.251	73.3	−0.3	0.753	72.8	0.2	−0.500	73.6	−0.6	0.992

logical sources may not form a bilayer phase (Luzzati and Husson, 1962), which could indicate that nonlamellar phases, and the Gaussian curvature energy, have important biological functions (Cullis and deKruijff, 1979). Except, maybe, in the case of bilayer fusion and vesicle budding, the biological role of nonbilayer structures remains elusive, and, as shown in the Appendix, the Gaussian curvature component to ΔG_{def} is negligible for inclusion-induced deformations. Moreover, the propensity to form nonbilayer structures cannot be the sole determinant of the bilayer control of membrane protein function because the function of membrane proteins is altered by maneuvers that primarily alter the propensity to form nonbilayer phases (Navarro et al., 1984; Brown, 1994; McCallum and Epand, 1995) or the bilayer thickness (Caffrey and Feigenson, 1981; Johannsson et al., 1981; Criado et al., 1984). In fact, ΔG_{CE} and ΔG_{SD} are comparable (Figs. 5, 7, and 9), and it is the sum of these interdependent contributions to ΔG_{def} that determines the bilayer component's modulation of membrane protein function. Descriptions that emphasize only the bilayer thickness or the curvature frustration will be incomplete.

The theory of elastic bilayer deformations provides a general framework for understanding how changes in lipid bilayer composition can modulate the function of integral membrane proteins. The apparent complexity of the theory, however, has been an obstacle for quantitative estimates of the bilayer deformation energy associated with conformational changes in membrane proteins, estimates that are needed to provide mechanistic insights. To overcome this obstacle we used a parametric description of the inclusion-induced deformation energy and its decomposition into two underlying components: the monolayer bending energy and the bilayer compression energy. This decomposition is a continuum approximation; but it constitutes a framework for analyzing inclusion-induced bilayer deformations that, subject to the choice of boundary conditions, is in good agreement with experimental results (Huang, 1986; Lundbæk and Andersen, 1999). The relevant deformation energies can be considerable, meaning that the bilayer material properties (and thus the bilayer lipid composition) can exert significant effects on protein function.

First, we discuss the issues of monolayer equilibrium curvature, boundary conditions, and scaling relations. Next, we discuss how the bilayer material properties can modulate membrane protein function. Finally, we briefly address some issues relating to multicomponent bilayers.

Boundary conditions, scaling relations, and monolayer equilibrium curvature

The present analysis confirms and extends previous theoretical studies (Huang, 1986; Helfrich and Jakobsson, 1990; Ring, 1996), which show that the bilayer deformation energy depends on the choice of boundary conditions at the inclusion/bilayer boundary. Experimental support for the coupling between the splay-distortion and compression-expansion components of ΔG_{def} was provided by Kirk and Gruner (1985), who showed that a modest amount of tetradecane shifts the lamellar $\rightarrow H_{II}$ transition temperature, T_c, of dioleoylphosphatidylethanolamine by ~30°C. This shift in T_c arises because tetradecane can redistribute freely within the system and thereby release the curvature stress by minimizing the lipid packing constraints, which include a compression-expansion energy component, in the H_{II} phase. In effect, the presence of tetradecane changes the boundary value problem from being constrained to being relaxed. A similar conclusion was reached by Lundbæk and Andersen (1999), based on analysis of the variation of the gA channel lifetime as a function of bilayer thickness.

That ΔG_{def} depends on the choice of boundary condition at r_0 should be expected because spectroscopic studies show that lipids adjacent to gramicidin channels (in bilayers with gramicidin/lipid mole fractions less than 1/15) are perturbed by the presence of the inclusion (Rice and Oldfield, 1979; Ge and Freed, 1993). Molecular dynamics studies similarly show that acyl chain motions are restricted by the inclusion, which causes the acyl-chain order parameter to increase and

TABLE 7 Parameterization of $\Delta G_{SD,c_0=0}$

i	$\bar{a}_{a,i}$	$\hat{a}_{a,i}$	$n_{a,i}$	$\bar{a}_{c,i}$	$\hat{a}_{c,i}$	$n_{c,i}$	$\bar{a}_{d,i}$	$\hat{a}_{d,i}$	$n_{d,i}$	$\bar{a}_{r,i}$	$\hat{a}_{r,i}$	$n_{r,i}$
1	101.9	5.1	0.698	91.6	4.0	0.395	103.0	4.0	−1.379	67.0	40.0	1.054
2	254.9	12.1	0.470	258.2	8.8	0.571	256.7	10.3	−0.933	240.9	26.1	0.872
3	221.5	−6.5	0.249	217.0	−2.0	0.738	221.8	−6.8	−0.497	223.8	−8.8	0.992

the chains to extend (Chiu et al., 1999). This perturbation of the local lipid dynamics and packing incurs an energetic cost, which is not included in the standard continuum analysis of ΔG_{def}.

Another uncertainty is whether one can justify the neglect of higher order terms in the expression for $\Delta G_{continuum}$ (Helfrich, 1981), and whether the continuum values of K_a and K_c are appropriate for describing bilayer deformations at the small length scales that pertain to inclusion-induced deformations (Helfrich, 1981; Partenskii and Jordan, 2000). That is, unless there is a fortuitous cancellation of errors, the bilayer deformation energy will differ from the conventional continuum contribution (as determined from Eq. 2, using Eqs. 3a–d).

In the present work, we maintain the framework provided by the continuum analysis, and we lump the above uncertainties together in our choice of boundary conditions, where we constrain the slope of the deformation profile at r_0. The particular choice for the constrained boundary condition (Eq. 3f) can be justified by noting the following: first, when $c_0 = 0$ the $s = 0$ condition is a limiting value based on geometric arguments of the constraints on the acyl chain motion; and second, the $s = 0$ condition leads to a spring constant that agrees with experimental results (Lundbæk and Andersen, 1999). In addition, we avoid introducing currently unknown, and therefore arbitrary, parameters to describe the energetics of the local lipid packing. Nevertheless, how well is this slope determined? A priori, the hydrophobic penalty for moving a phospholipid molecule into or out of the bilayer by ~0.07 nm, corresponding to one CH_2 in each acyl chain, is ~2.3kT, meaning that the membrane-solution interface is dynamic. Neutron diffraction, x-ray, and molecular dynamics studies show, in fact, that the membrane-solution interface fluctuates (Wiener and White, 1992; Woolf and Roux, 1996), and both the unperturbed and perturbed bilayer thicknesses denote average values. Other measured bilayer properties, including K_a and K_c, similarly are average values. Molecular dynamic simulations show, however, that the local fluctuations close to an inclusion are less than those in the unperturbed bilayer (Petrache et al., 2000), which suggests that one can define a slope for the deformation profile at r_0, even if the precision with which the slope is known depends on the time scale of interest.

The monolayer equilibrium curvature and the bilayer material moduli are determined by the profile of intermolecular forces through the component monolayers (e.g., Helfrich, 1973; Helfrich, 1981; Petrov and Bivas, 1984; Seddon, 1990). Lipid packing adjacent to an inclusion will be determined by the intermolecular interactions at the inclusion/bilayer boundary. The overall effects of the profile of intermolecular interactions often is expressed in terms of the effective molecular "shape" of the component lipids (e.g., Seddon, 1990), which in turn can be related to the monolayer equilibrium curvature. In the absence of knowledge about the interactions between the inclusion and the surrounding lipids, we assume they are similar to the interactions among lipid molecules. This is equivalent to assuming that the unperturbed shape of the annular lipids is similar to that of the bulk lipids in a relaxed monolayer.

The lipid organization at the inclusion/bilayer boundary is constrained by the requirement that there cannot be a void at the boundary. The value of s therefore will be determined, in part, by the energetic penalty associated with having a tilt between the bilayer normal and the director for the acyl chains. (Specifically, there will be a restriction on the director along r. The acyl chains should be free to move perpendicular to r; but their average position should average out.) Limiting the discussion to cylindrical inclusions: when $c_0 = 0$, the lipids are effectively cylindrical and, if the penalty for tilt is significant, then $s \approx 0$ (Eq. 3e). When $c_0 \neq 0$, the lipid effective shape is not cylindrical and a perfect alignment implies that $s \neq 0$. If there were no constraints on lipid packing, the slope at the inclusion/bilayer boundary would be determined by Eq. 3d. If there are constraints on lipid packing, s can be approximated based on simple geometric arguments (Eq. 3f). The actual value of s (for $c_0 \neq 0$) could differ from the estimate based on Eq. 3f because, for any value of c_0 (and any shape of the unperturbed lipid), the effective lipid shape in an unperturbed planar bilayer will be cylindrical (e.g., Andersen et al., 1999). That is, the lipid molecules can change "shape." Similar changes in lipid shape could occur at the inclusion/bilayer boundary, in which case s, and ΔG_{def}, will be somewhere between the limiting estimates we provide.

In the biquadratic expression for $\Delta G_{def,c_0=0}$ (Eq. 9), the coefficients a_1, a_2, and a_3 are determined by the bilayer mechanical properties (K_a, K_c, and d_0) and the inclusion radius r_0 but are independent of boundary conditions. The boundary condition dependence of $\Delta G_{def,c_0=0}$ arises because different combinations of a_1, a_2, and a_3 will determine the energy (for a fixed u_0). Importantly, values for a_1, a_2, and a_3 can be estimated for other inclusion/lipid systems using the scaling relations (Eq. 37–39). Because ΔG_{MEC} is included in ΔG_{def} by simple addition (Eq. 8), it is possible to obtain a complete and general solution to the energetic consequences of inclusion-induced bilayer deformations.

The difference in ΔG_{def} for the two boundary conditions (Fig. 5 versus Figs. 7 *a* and Fig. 9 *b*) is that the curvature stress, the $\pi\int K_c c_0^2 r\, dr$ contribution to ΔG_{def}, cannot be tapped effectively in the case of the constrained boundary condition, where the local curvature required to eliminate voids in lipid packing adjacent to the inclusion will be of a sign opposite that of c_0, and $\Delta G_{MEC}^{con} = 2\pi K_c c_0^2 r_0 R_{Head}$ will always be greater than or equal to 0.

When ΔG_{def} is evaluated using either boundary condition ($s = R_{Head}c_0$ or $s = s_{min}$), the relation between ΔG_{def} and c_0 depends on the assumption one makes for u_0. For physiologically relevant situations, u_0 is invariant with respect to changes in c_0 and ΔG_{def} is a second-order polynomial in c_0 (Eqs. 17 and 28). Only when u_0 varies as a function of c_0

will ΔG_{def} be a quadratic function of c_0 (Eqs. 18b and 29b). Even then, the $\Delta G_{def}(c_0)$ relations differ from predictions based on the $K_c c_0^2/2$ energy density. Most of the deformation energy is due to the bilayer deformation within the first annulus of lipid molecules around the inclusion (Nielsen et al., 1998), i.e., within an area approximately equal to $4\pi r_0 R_0$ (17 nm^2 for the reference inclusion). For $c_0 = 0.1$ nm^{-1}, $K_c c_0^2/2 = 0.11kT/nm^2$ for SOPC bilayers, and the local curvature stress in the first annulus is $1.9kT$. For comparison, if $u_0 = 0.1$ nm then $\Delta G_{MEC}^{rel} = -6.6kT$ (and $\Delta G_{def}^{rel} = -3.7kT$) and ΔG_{MEC}^{con} $(=2\pi K_c c_0^2 r_0 R_0) = 2.0kT$ (and $\Delta G_{def}^{con} = 8.6kT$).

Lipid bilayer mechanics, boundary conditions, and protein function

Both $\Delta\Delta G_{def}^{rel}(0 \rightarrow u_0|_{min})$ (Eq. 20) and $\Delta\Delta G_{def}^{con}(0 \rightarrow u_0|_{min})$ (Eq. 31) are less than or equal to 0, which means that the curvature stress associated with a $c_0 \neq 0$ can "drive" protein conformational changes. For the relaxed boundary condition, a $c_0 > 0$ promotes a local inclusion-induced bilayer thinning (Fig. 7 *b*). For the constrained boundary condition, a $c_0 > 0$ will impede this local thinning (Fig. 9 *b*). In either case, the value of u_0 for which $\Delta G_{def}(u_0)$ is a minimum will be proportional to c_0, and the minimum value of ΔG_{def} will be proportional to c_0^2; but one cannot predict how changes in c_0 will affect membrane proteins without knowing the applicable boundary condition.

To illustrate the coupling between bilayer mechanics and protein function, we note that the conformational changes that occur in the bilayer-spanning part of integral membrane proteins most likely involve sliding or tilting motions between transmembrane helices (or domains) (Unwin, 1989; Kaback and Wu, 1997; Sakmar, 1998). The close ↔ open transition in gap junction channels, for example, involves a tilt of the domains by 7–8° (Unwin and Ennis, 1984), corresponding to a length change of ~0.3 Å. Both the closed and open states are likely to perturb the surrounding bilayer, with bilayer deformation energies $\Delta G_{def,c}$ and $\Delta G_{def,o}$, and the bilayer-dependent contribution to the free energy change of the close ↔ open transition is

$$\Delta\Delta G_{def} = \Delta G_{def,o} - \Delta G_{def,c}, \quad (40)$$

The channel open probability (P_O) is

$$P_O = \frac{1}{1 + K^*_{c\leftrightarrow o}\exp(\Delta\Delta G_{def}/kT)}, \quad (41)$$

where $K^*_{c\leftrightarrow o}$ is the intrinsic equilibrium constant of the close↔open transition. Equations 40 and 41 provide for a mechanistic link between the bilayer material properties and membrane protein function.

The energetic consequences of changes in monolayer equilibrium curvature are qualitatively different for the relaxed and the constrained boundary conditions (see Results). This difference is striking when the equilibrium distribution between different protein conformations is examined, where one needs to know how $\Delta G_{def,o}$, $\Delta G_{def,c}$, and $\Delta\Delta G_{def}(=\Delta G_{def,o} - \Delta G_{def,c})$ vary as a function of c_0. Consider a protein conformational change similar to the open ↔ close transition in a gap junction channel (Table 3).

For the relaxed boundary condition,

$$\Delta\Delta G_{def}^{rel}(c_0) = \left(\frac{a_2\pi K_c r_0(l_o - l_c)}{2a_3}\right)c_c + \left(a_1 - \frac{a_2^2}{4a_3}\right) \cdot \left(\frac{(l_o + l_c - 2d_0)(l_o - l_c)}{4}\right). \quad (42)$$

$\Delta\Delta G_{def}^{rel}$ is composed of two terms: a c_0-dependent term, which is not explicitly d_0-dependent (a_2 and a_3 vary with d_0) and varies as a function of $l_o - l_c$, the difference in length between the two conformations; and a d_0 (and $l_o - l_c$)-dependent term, which does not depend on c_0.

When $d_0 = 2.8$ nm (and $c_0 = 0$), $\Delta G_{def,o}^{rel} < \Delta G_{def,c}^{rel}$ and $\Delta\Delta G_{def}^{rel} < 0$, as the shorter (open) conformation causes a smaller bilayer deformation than the longer conformation. When $d_0 = 3.0$ nm (and $c_0 = 0$), $\Delta G_{def,o}^{rel} = \Delta G_{def,c}^{rel}$ and $\Delta\Delta G_{def,c_0}^{rel} = 0 = 0$, as the two conformations give rise to the same deformation energy. When $d_0 = 3.2$ nm (and $c_0 = 0$), $\Delta G_{def,o}^{rel} > \Delta G_{def,c}^{rel}$ and $\Delta\Delta G_{def,c_0}^{rel} = 0 > 0$, as the open conformation causes a larger bilayer deformation than the closed conformation.

For the constrained boundary condition,

$$\Delta\Delta G_{def}^{con} = -\left(\frac{R_{Head}a_2(l_o - l_c)}{2}\right)c_0 + a_1\left(\frac{(l_o + l_c - 2d_0)(l_o - l_c)}{4}\right). \quad (43)$$

When $c_0 = 0$, the $\Delta\Delta G_{def}^{con}(d_0)$ changes will be similar to, but of larger magnitude than, the changes in $\Delta\Delta G_{def}^{rel}(d_0)$. The qualitative dependence of $\Delta\Delta G_{def}^{con}$ on d_0 is similar to that of $\Delta\Delta G_{def}^{rel}$, but the c_0-dependent contribution to $\Delta\Delta G_{def}^{con}$ has a sign opposite that of $\Delta\Delta G_{def}^{rel}$ and does not depend explicitly on K_c (there is an implicit K_c dependence, which arises from the K_c dependence of a_2). It is important to know the applicable boundary condition at r_0 before predicting the effects of a change in monolayer equilibrium curvature on protein function.

For either boundary condition, a $c_0 \neq 0$ will alter both $\Delta G_{def,o}$ and $\Delta G_{def,c}$ (and $\Delta\Delta G_{def}$) and hence the equilibrium distribution between the two conformations. Because $\Delta\Delta G_{def}$ is a linear function of c_0 (cf. Eqs. 42 and 43), with a slope proportional to $l_o - l_c$, a given change in c_0 will have different consequences for different membrane proteins.

The importance of the boundary condition is illustrated in Fig. 12, which shows how $\Delta\Delta G_{def}$ and P_O (Eq. 41) vary as functions of c_0. Fig. 12, *a* and *b*, shows results for the

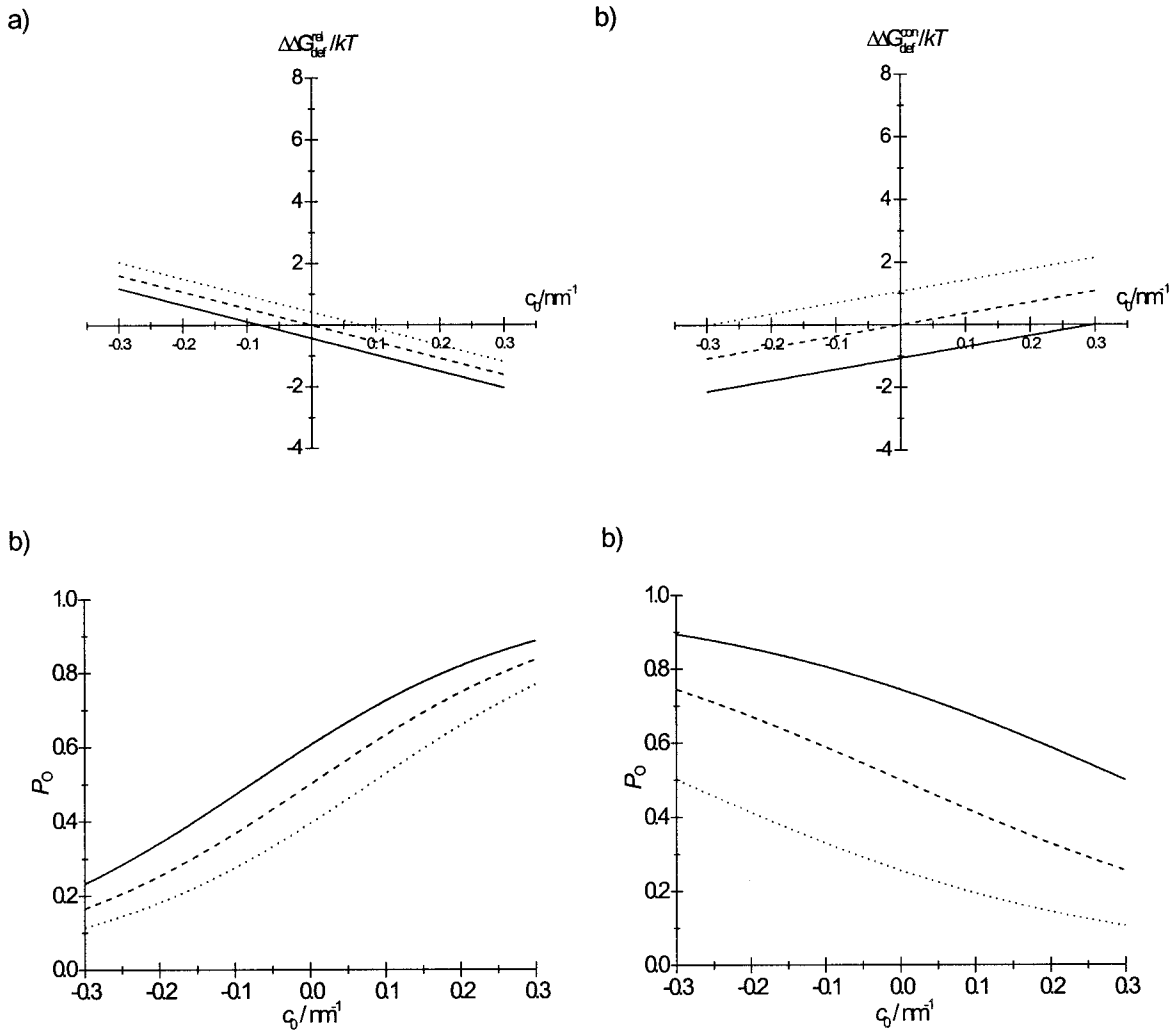

FIGURE 12 $\Delta\Delta G_{def}$ (Eqs. 42 and 43) and P_O (Eq. 41) as functions of c_0 and d_0 for a gap junction-like protein with $l_o - l_c = -0.03$ nm. (*a*) $\Delta\Delta G^{rel}_{def}$ with $d_0 = 2.8$ (—), $d_0 = 3.0$ (– –), and $d_0 = 3.2$ nm (· · · · · ·). (*b*) The associated P_O; as in *a*. (*c*) $\Delta\Delta G^{con}_{def}$; as in *a*. (*d*) The associated P_O; as in *a*.

relaxed boundary condition (Eqs. 41 and 42). When $c_0 = 0$, a change in u_0 by only 0.2 nm has a measurable effect on the closed ↔ open equilibrium (or P_O); similar effects occur for $c_0 \neq 0$. Fig. 12, *c* and *d*, shows results for the constrained boundary condition (Eqs. 41 and 43). The opposite slopes of the $\Delta\Delta G^{rel}_{def}(c_0)$ and $\Delta\Delta G^{con}_{def}(c_0)$ relations are reflected in the different behavior of the $P_O(c_0)$ relations. When $c_0 = 0$, the equilibrium distribution between the two conformational states is more sensitive to changes in bilayer thickness in the case of the constrained as compared to the relaxed boundary condition.

Cholesterol addition increases K_a and K_c of SOPC bilayers (Needham and Nunn, 1990) and changes d_0 and c_0 as well (Tilcock et al., 1984; Nezil and Bloom, 1992). We can evaluate how these changes in bilayer properties alter ΔG_{def} and $\Delta\Delta G_{def}$, using the scaling relations (Eqs. 37–39); the results are in good agreement with the directly calculated results (Fig. 13). As one would expect, the presence of cholesterol alters the c_0 dependence of the equilibrium distribution between protein conformational states in a manner that depends on the boundary condition at r_0.

For the relaxed boundary condition, the addition of cholesterol (1:1) to SOPC preserves the general features of the $\Delta\Delta G^{rel}_{def}(c_0)$ relation as compared with the SOPC bilayer (Fig. 13 *a*) but shifts the midpoint of the $P_O(c_0)$ relation toward positive c_0 (Fig. 13 *b*). For a DOPC bilayer, the smaller values for the mechanical moduli lead to an increased sensitivity to c_0, as compared with SOPC (Fig. 13 *a*). In addition, the decrease in d_0 shifts the midpoint for the $P_O(c_0)$ relation toward negative c_0, because the second (constant) terms in Eqs. 40 and 41 are nonzero when $d_0 \neq 3.0$ nm (Fig. 13 *b*). For the constrained boundary condition, the addition of cholesterol (1:1) to SOPC increases the sensitivity of the $\Delta\Delta G^{con}_{def}(c_0)$ relation as compared with the pure SOPC bilayer (Fig. 13 *c*) and shifts the midpoint of the $P_O(c_0)$ relation toward negative c_0 (Fig. 13 *d*). For a DOPC

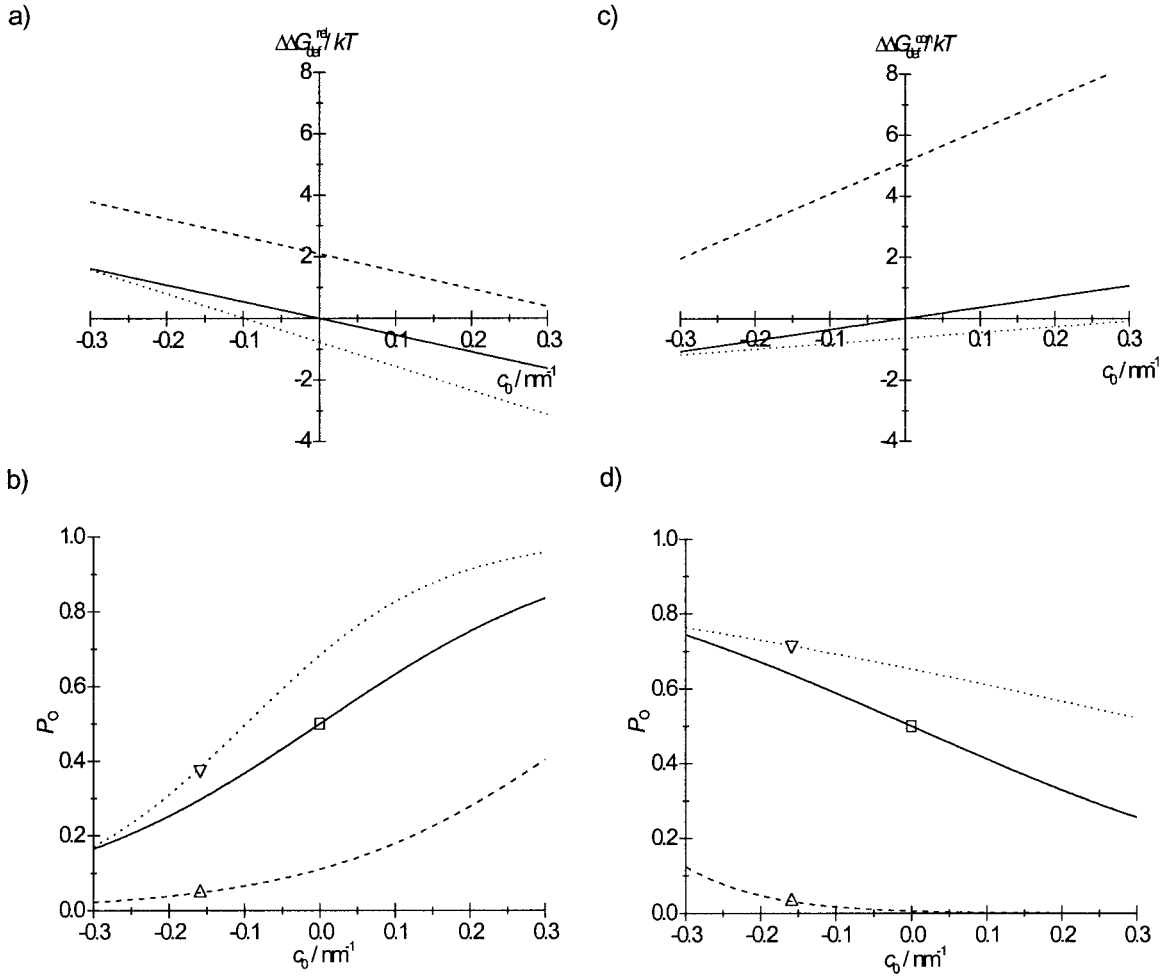

FIGURE 13 Bilayer deformation energy and membrane protein function. The $\Delta\Delta G_{def}(c_0)$ and $P_O(c_0)$ relations were calculated using Eqs. 40–43 and the scaling relations Eqs. 37–39. (*a*) $\Delta\Delta G_{def}^{rel}(c_0)$ for $l_o - l_c = -0.03$ nm in SOPC, $d_0 = 3.0$ nm (—); SOPC:Chol, $d_0 = 3.3$ nm (– –); and DOPC, $d_0 = 2.6$ nm (· · · · · ·). (*b*) $P_0(c_0)$ relations determined using the $\Delta\Delta G_{def}^{rel}(c_0)$ values in *a* (curves as in *a*). (*c* and *d*) The corresponding $\Delta\Delta G_{def}^{con}(c_0)$ and associated $P_o(c_0)$ relations (curves as in *a*). The three points in *b* and *d* denote the specific solutions for $c_0 = 0$ for SOPC (indicated by □); $c_0 = -0.16$ nm^{-1} for SOPC:Chol (indicated by △); and $c_0 = -0.16$ nm^{-1} for DOPC (indicated by ▽) (the c_0 values for SOPC:Chol were estimated from the method of Rand and Parsegian (1997)).

bilayer, the sensitivity of the $\Delta\Delta G_{def}^{con}(c_0)$ relation is decreased as compared with SOPC (Fig. 13 *b*), and the midpoint for the $P_O(c_0)$ relation is shifted toward positive c_0 (Fig. 13 *d*).

For either boundary condition, $\Delta\Delta G_{def}$ is composed of a c_0-dependent and a c_0-independent term (Eqs. 42 and 43). For constant r_0, the curvature-dependent terms are linear in c_0; but the slope of the relation will vary as a function of the inclusion dimensions, the bilayer mechanical properties, and the choice of boundary conditions. The c_0-independent terms in Eqs. 17 and 27 are identical to Eqs. 11a and 13a, and the c_0-independent contributions to $\Delta\Delta G_{def}$ (Eqs. 42 and 43) are identical to the corresponding expressions derived from Eqs. 11a and 13b. That is, it is possible to determine the spring constant experimentally, using the methods described by Andersen et al. (1999) and Lundbæk and Andersen (1999).

Changes in d_0 have only modest effects on the c_0 dependence of $\Delta\Delta G_{def}$ (Eqs. 42 and 43) because the d_0 dependence of the c_0-dependent term is introduced only through a_3, which is a weak function of d_0 (Table 5). Nevertheless, changes in d_0 may shift the inflection point of the $P_O(c_0)$ curves, because of changes in u_0. This is seen in Fig. 13, where the open gap junction channel produces the least deformation in DOPC bilayers, as compared with SOPC and SOPC:Chol bilayers. Consequently, $P_O(0)$ is highest in DOPC bilayers. This coupling between the effects of c_0 and d_0 (or u_0) on $\Delta\Delta G_{def}$ shows that the bilayer is a, perhaps surprising, dynamic environment.

Finally, ΔG_{MEC} can be interpreted as a line tension that will tend to increase or decrease r_0 (Dan and Safran, 1998). Should the curvature-dependent changes in ΔG_{def} be interpreted as being due to a lateral pressure imposed on the protein by the bilayer rather than the bilayer compression?

Given that a change in c_0 results from a change in the profile of intermolecular forces through each monolayer, which usually also will alter K_a and K_c, a change in c_0 will be associated with a change in the lateral pressure exerted on the protein (Cantor, 1997, 1999). These changes in lateral pressure, however, have a minimal impact on ΔG_{def} (or $\Delta\Delta G_{def}$) unless r_0 changes dramatically. For nonisovolumic changes, such as the opening and closing of mechanosensitive channels, the consequences of the resulting change in r_0 can be evaluated from the scaling relation in Eq. 38: a 10% change in r_0 relative to the reference situation (cf. Sukharev et al., 1999) will change ΔG_{def} by less than 7%. That is, the u_0-dependent changes in ΔG_{def} will dominate the r_0-dependent changes.

Multicomponent bilayers

The present analysis depends on the assumption that the bilayer can be treated as a uniform homogeneous, single-component continuum. Multicomponent bilayers have additional degrees of freedom, which may contribute to the minimization of ΔG_{def} by allowing for a ΔG_{def}-driven lipid redistribution close to the inclusion. This is particularly important for the constrained boundary condition, where the magnitude of ΔG_{def} easily becomes so large that it could cause a significant, local redistribution of the bilayer components, which would tend to reduce the magnitude of ΔG_{def}. For solvent-containing bilayers, the packing constraints would be relieved by the redistribution of solvent molecules (cf. Kirk and Gruner, 1985), in which case the appropriate boundary condition should be close to $s = s_{min}$ (Lundbæk and Andersen, 1999). In the case of bilayers made of lipids of different length or shape, the ΔG_{def} could be minimized by a local accumulation of lipids that pack optimally around the inclusion (Maer et al., 1999). Care must be taken when evaluating the effects of boundary conditions and monolayer equilibrium curvature on ΔG_{def} in multicomponent bilayers. It is necessary to have experimental determinations of the bilayer response to well-defined inclusion-induced deformations. Eventually, it will be necessary to approach the problem of protein-bilayer interactions by explicitly incorporating not only the (static and dynamic) details of lipid packing at the protein-bilayer boundary, but also the radial distribution of the different membrane components around the protein in question (cf. Sperotto and Mouritsen, 1993).

APPENDIX

The Gaussian curvature ΔG_{GC} can be evaluated as a function of s (Ring, 1996):

$$\Delta G_{GC} = \pi\overline{K_c}\int_{r_0}^{\infty} c_1 c_2 r\, dr = \frac{\pi}{2}\overline{K_c}\frac{s^2}{1+s^2}. \qquad (A1)$$

$\overline{K_c}/K_c$ has been estimated to be 0.048 in a 2:1 (mol:mol) hydrated mixture of lauric acid and dilauroylphosphatidylcholine in the bicontinuous *Im*3*m* (Q^{229}) phase at 60°C (Templer et al., 1994). For hydrated glycerolmonooleate in the *Ia*3*d* (Q^{230}) phase, $\overline{K_c}/K_c = 0.032$ at 35°C (Chung and Caffrey, 1994). Making use of the fact that the available experimental estimates of $\overline{K_c}/K_c \le 0.05$,

$$\Delta G_{GC} = \frac{\pi}{2}\overline{K_c}\left(\frac{s^2}{1+s^2}\right) \le \frac{\pi}{2}0.05K_c\left(\frac{s^2}{1+s^2}\right). \qquad (A2)$$

For $s = 0$, $\Delta G_{GC} \equiv 0$; for $s = s_{min}$, ΔG_{GC} can be expressed using Eq. 12:

$$\Delta G_{GC} \le \frac{\pi}{2}0.05K_c\left(\frac{(u_0 a_2/2a_3)^2}{1+(u_0 a_2/2a_3)^2}\right) < \pi\cdot 0.025K_c(a_2/2a_3)^2u_0^2. \qquad (A3)$$

The rightmost part of A3 has the form of Eq. 14, but with an apparent spring constant that is $\pi K_c(a_2/a_3)^2/640$ (or $\sim 0.3kT/nm^2$ for SOPC bilayers). This value should be compared with the spring constants derived from the SOPC moduli ($H_B^{con} = 88.8kT/nm^2$ and $H_B^{rel} = 35.6kT/nm^2$; see text). The Gaussian curvature energy contribution to ΔG_{def} will be <1%. Even if $\bar{K}_c$ were underestimated by an order of magnitude, ΔG_{GC} would be a modest contribution to ΔG_{def}; one can disregard contributions from the Gaussian curvature and limit the analysis to the effects of the mean curvature only.

We thank Drs. R. Cantor, M. Goulian, J. A. Lundbæk, M. B. Partensky, and D. Siegel for helpful discussions and the referees for constructive suggestions for improving the manuscript.

The present work was supported by National Institutes of Health grant GM21342 (OSA), a Danish Natural Science Research Council SNF grant (11-1219-1 to CN), a Winston Fellowship (CN), and a Carlsberg Foundation Research grant (20-1249 to CN).

REFERENCES

Andersen, O. S., C. Nielsen, A. M. Maer, J. A. Lundbæk, M. Goulian, and R. E. Koeppe, II. 1999. Ion channels as tools to monitor lipid bilayer-membrane protein interactions: gramicidin channels as molecular force transducers. *Methods Enzymol.* 294:208–224.

Benz, R., and K. Janko. 1976. Voltage-dependent capacitance relaxation of lipid bilayer membranes. Effects of membrane composition. *Biochim. Biophys. Acta.* 455:721–738.

Bezrukov, S., R. P. Rand, I. Vodyanoy, and V. A. Parsegian. 1998. Lipid packing stress and polypeptide aggregation: alamethicin channel probed by proton titration of lipid charge. *Faraday Discuss.* 111:173–183.

Bezrukov, S. M., I. R. P. Vodyanoy, and V. A. Parsegian. 1995. pH induced variations in lipid packing stress may correlate with relative probabilities of alamethicin conductance states. *Biophys. J.* 68:A341.

Brown, M. F. 1994. Modulation of rhodopsin function by properties of the membrane bilayer. *Chem. Phys. Lipids.* 73:159–180.

Caffrey, M., and G. W. Feigenson. 1981. Fluorescence quenching in model membranes. 3. Relationship between calcium adenosinetriphosphatase enzyme activity and the affinity of the protein for phosphatidylcholines with different acyl chain characteristics. *Biochemistry.* 20:1949–1961.

Cantor, R. 1997. Lateral pressures in cell membranes: a mechanism for modulation of protein function. *J. Phys. Chem. B.* 101:1723–1725.

Cantor, R. 1999. Lipid composition and the lateral pressure profile in bilayers. *Biophys. J.* 76:2625–2639.

Chiu, S. W., L. K. Nicholson, M. T. Brenneman, S. Subramaniam, Q. Teng, J. A. McCammon, T. A. Cross, and E. Jakobsson. 1991. Molecular dynamics computations and solid state nuclear magnetic resonance of the gramicidin cation channel. *Biophys. J.* 60:974–978.

Chiu, S.-W., S. Subramaniam, and E. Jakobsson. 1999. Simulation study of a gramicidin/lipid bilayer system in excess water and lipid. I. Structure of the molecular complex. *Biophys. J.* 76:1929–1938.

Chung, H., and M. Caffrey. 1994. The curvature elasticity-energy function of the lipid-water cubic mesophase. *Nature.* 368:224–226.

Criado, M., H. Eibl, and F. J. Barrantes. 1984. Functional properties of the acetylcholine receptor incorporated in model lipid membranes. Differential effects of chain length and head group of phospholipids on receptor affinity states and receptor-mediated ion translocation. *J. Biol. Chem.* 259:9188–9198.

Cullis, P. R., and B. deKruijff. 1979. Lipid polymorphism and the functional roles of lipids in biological membranes. *Biochim. Biophys. Acta.* 559:399–420.

Dan, N., and S. A. Safran. 1998. Effect of lipid characteristics on the structure of transmembrane proteins. *Biophys. J.* 75:1410–1414.

Deisenhofer, J., O. Epp, K. Miki, R. Huber, and H. Michel. 1985. Structure of the protein subunits in the photosynthetic reaction centre of *Rhodopseudomonas viridis* at 3-Å resolution. *Nature.* 318:618–624.

Doyle, D. A., J. M. Cabral, R. A. Pfuetzner, A. Kuo, J. M. Gulbis, S. L. Cohen, B. T. Chait, and R. MacKinnon. 1998. The structure of the potassium channel: molecular basis of K^+ conduction and selectivity. *Science.* 280:69–77.

Elliott, J. R., D. Needham, J. P. Dilger, and D. A. Haydon. 1983. The effects of bilayer thickness and tension on gramicidin single-channel lifetime. *Biochim. Biophys. Acta.* 735:95–103.

Epand, R., editor. 1997. Lipid Polymorphism and Membrane Properties. Academic Press, San Diego. 1–568.

Evans, E. A., and R. M. Hochmuth. 1978. Mechanochemical properties of membranes. *Curr. Top. Membr. Transp.* 10:1–64.

Evans, E., and D. Needham. 1987. Physical properties of surfactant bilayer membranes: thermal transitions, elasticity, rigidity, cohesion, and colloidal interactions. *J. Phys. Chem.* 91:4219–4228.

Evans, E., and W. Rawicz. 1990. Entropy-driven tension and bending elasticity in condensed fluid membranes. *Phys. Rev. Lett.* 64: 2094–2097.

Evans, E., W. Rawicz, and A. F. Hofmann. 1995. Lipid bilayer expansion and mechanical disruption in solutions of water-soluble bile acid. *In* Bile Acids in Gastroenterology Basic and Clinical Advances. A. F. Hofmann, G. Paumgartner, and A. Stiehl, editors. Kluwer Academic, Dordrecht. 59–68.

Ge, M., and Freed, J. H. 1993. An electron spin resonance study of interactions between gramidicin A and phosphatidylcholine bilayers. *Biophys. J.* 65:2106–2123.

Gruner, S. M. 1985. Intrinsic curvature hypothesis for biomembrane lipid composition: a role for nonbilayer lipids. *Proc. Natl. Acad. Sci. USA.* 82:3665–3669.

Gruner, S. M. 1991. Lipid membrane curvature elasticity and protein function. *Biologically Inspired Phys.* 127–135.

Hazel, J. R. 1995. Thermal adaption in biological membranes: is homeoviscous adaption the explanation? *Annu. Rev. Physiol.* 57:19–42.

Helfrich, P., and E. Jakobsson. 1990. Calculation of deformation energies and conformations in lipid membranes containing gramicidin channels. *Biophys. J.* 57:1075–1084.

Helfrich, W. 1973. Elastic properties of lipid bilayers: theory and possible experiments. *Z. Naturforsch.* 28C:693–703.

Helfrich, W. 1981. Amphiphilic mesophases made of defects. *In* Physique des défauts (Physics of Defects). R. Balian, M. Kléman, and J.-P. Poirier, editors. North-Holland Publishing, New York. 716–755.

Henderson, R., J. M. Baldwin, T. A. Ceska, F. Zemlin, E. Beckmann, and K. H. Downing. 1990. Model for the structure of bacteriorhodopsin based on high-resolution electron cryomicroscopy. *J. Mol. Biol.* 213: 899–929.

Hladky, S. B., and D. W. R. Gruen. 1982. Thickness fluctuations in black lipid membranes. *Biophys. J.* 38:251–258.

Huang, H. W. 1986. Deformation free energy of bilayer membrane and its effect on gramicidin channel lifetime. *Biophys. J.* 50:1061–1070.

Hui, S. W. 1997. Curvature stress and biomembrane function. *Curr. Top. Membr.* 44:541–563.

Johannsson, A., G. A. Smith, and J. C. Metcalfe. 1981. The effect of bilayer thickness on the activity of $(Na^{++}K^+)$-ATPase. *Biochim. Biophys. Acta.* 641:416–421.

Kaback, H. R., and J. Wu. 1997. From membrane to molecule to the third amino acid from the left with a membrane transport protein. *Q. Rev. Biophys.* 30:333–364.

Keller, S. L., S. M. Bezrukov, S. M. Gruner, M. W. Tate, I. Vodyanoy, and V. A. Parsegian. 1993. Probability of alamethicin conductance states varies with nonlamellar tendency of bilayer phospholipids. *Biophys. J.* 65:23–27.

Kirk, G. L., and S. M. Gruner. 1985. Lyotropic effects of alkanes and headgroup composition on the $L\alpha$-H_{II} lipid crystal phase transition: hydrocarbon packing versus intrinsic curvature. *J. Physique.* 46: 761–769.

Landau, L. D., and E. M. Lifshitz. 1986. Theory of Elasticity. Butterworth-Heinemann, Oxford.

Lindblom, G., J. B. Haukson, L. Rilfors, B. Bergenstål, Å. Wieslander, and P.-O. Eriksson. 1993. Membrane lipid regulation in *Acholeplasma laidlawii* grown with saturated fatty acids. Synthesis of a triacyl glucolipid not forming liquid crystalline structures. *J. Biol. Chem.* 268: 16198–16207.

Lundbæk, J. A., and O. S. Andersen. 1994. Lysophospholipids modulate channel function by altering the mechanical properties of lipid bilayers. *J. Gen. Physiol.* 104:645–673.

Lundbæk, J., and O. S. Andersen. 1999. Spring constants for channel-induced lipid bilayer deformations—estimates using gramicidin channels. *Biophys. J.* 76:889–895.

Lundbæk, J. A., P. Birn, J. Girshman, A. J. Hansen, and O. S. Andersen. 1996. Membrane stiffness and channel function. *Biochemistry.* 35: 3825–3830.

Lundbæk, J. A., A. M. Maer, and O. S. Andersen. 1997. Lipid bilayer electrostatic energy, curvature stress, and assembly of gramicidin channels. *Biochemistry.* 36:5695–5701.

Luzzati, V., and F. Husson. 1962. The structure of the liquid-crystalline phases of lipid-water systems. *J. Cell. Biol.* 12:207–219.

Maer, A. M., C. Nielsen, and O. S. Andersen. 1999. Gramicidin channels in bilayers formed from phosphatidylcholine mixtures with a constant average number of methylene groups per lipid molecule. *Biophys. J.* 76:A213.

Marsh, D. 1990. CRC Handbook of Lipid Bilayers. CRC Press, Boca Raton, FL.

McCallum, C. D., and R. M. Epand. 1995. Insulin receptor autophosphorylation and signalling is altered by modulation of membrane physical properties. *Biochemistry.* 34:1815–1824.

Navarro, J., M. Toivio-Kinnucan, and E. Racker. 1984. Effect of lipid composition on the calcium/adenosine 5′-triphosphate coupling ratio of the Ca^{2+}-ATPase of sarcoplasmic reticulum. *Biochemistry.* 23:130–135.

Needham, D. 1995. Cohesion and permeability of lipid bilayer vesicles. *In* Permeability and Stability of Lipid Bilayers. E. A. Disalvo and S. A. Smon, editors. CRC Press, Boca Raton, FL. 49–76.

Needham, D., and R. S. Nunn. 1990. Elastic deformation and failure of lipid bilayer membranes containing cholesterol. *Biophys. J.* 58: 997–1009.

Nezil, F. A., and M. Bloom. 1992. Combined influence of cholesterol and synthetic amphiphilic peptides upon bilayer thickness in model membranes. *Biophys. J.* 61:1176–1183.

Nielsen, C., M. Goulian, and O. S. Andersen. 1998. Energetics of inclusion-induced bilayer deformations. *Biophys. J.* 74:1966–1983.

Niggemann, G., M. Kummrow, and W. Helfrich. 1995. The bending rigidity of phosphoatidylcholine bilayers: dependences on experimental method, sample cell sealing and temperature. *J. Physique II (France).* 5:413–425.

Owicki, J. C., M. W. Springgate, and H. M. McConnell. 1978. Theoretical study of protein-lipid and protein-protein interactions in bilayer membranes. *Proc. Natl. Acad. Sci. USA.* 75:1616–1619.

Partenskii, M. B., and P. C. Jordan. 2000. A non-local approach to peptide insertion in lipid bilayers. *Biophys. J.* 78:325A.

Perozo, E., D. M. Cortes, and L. G. Cuello. 1998. Three-dimensional architecture and gating mechanism of a K^+ channel studied by EPR spectroscopy. *Nature Struct. Biol.* 5:459–469.

Petrache, H. I., J. A. Killian, R. E. Koeppe, II, and T. B. Woolf. 2000. Interactions of WALP peptides with bilayers: molecular dynamics simulations. *Biophys. J.* 78:324A.

Petrov, A. G., and I. Bivas. 1984. Elastic and fexoelectric aspects of out-of-plane fluctuations in biological and model membranes. *Prog. Surf. Sci.* 16:389–512.

Rand, R. P., N. L. Fuller, S. M. Gruner, and V. A. Parsegian. 1990. Membrane curvature, lipid segregation, and structural transitions for phospholipids under dual-solvent stress. *Biochemistry.* 29:76–87.

Rand, R. P., and V. A. Parsegian. 1997. Hydration, curvature and bending elasticity of phospholipid monolayers. Lipid polymorphism and membrane properties. *Curr. Top. Membr.* 44:167–189.

Rawicz, W., K. O. Olbrich, T. McIntosh, D. Needham, and E. Evans. 2000. Effect of chain length and unsaturation on elasticity of lipid bilayers. *Biophys. J.* 79:328–339.

Rice, D, and E. Oldfield. Deuterium nuclear magnetic resonance studies of the interaction between dimyristoylphosphatidylcholine and gramicidin A. *Biochemistry*. 18:3272–327.

Rietveld, A. G., J. A. Killian, W. Dowhan, and B. de Kruijff. 1993. Polymorphic regulation of membrane phospholipid composition in *Escherichia coli*. *J. Biol. Chem.* 268:12427–12433.

Rilfors, L., Å. Wieslander, and G. Lindblom. 1993. Regulation and Physical Properties of the Polar Lipids in *Acholeplasma laidlawii*. *Subcell. Biochem.* 20:109–166.

Ring, A. 1996. Deformation free energy of bilayer membrane and its effects on gramicidin channel lifetime. *Biochim. Biophys. Acta.* 1278: 147–159.

Sadoc, J. F., and J. Charvolin. 1986. Frustration in bilayers and topologies of fluid crystals of amphiphilic molecules. *J. Physique.* 47:683–691.

Sakmar, T. P. 1998. Rhodopsin: a prototypical G protein-coupled receptor. *Prog. Nucleic Acid Res. Mol. Biol.* 59:1–34.

Seddon, J. M. 1990. Structure of the inverted hexagonal (H^{II}) phase, and non-lamellar phase transitions of lipids. *Biochim. Biophys. Acta.* 1031: 1–69.

Sperotto, M. M., and O. G. Mouritsen. 1993. Lipid enrichment and selectivity of integral membrane proteins in two component lipid bilayers. *Eur. Biophys. J.* 22:323–328.

Sukharev, S. I., W. J. Sigurdson, C. Kung, and F. Sachs. 1999. Energetic and spatial parameters for gating of the bacterial large conductance mechanosensitive channel MscL. *J. Gen. Physiol.* 113:525–539.

Templer, R. H., J. M. Seddon, and N. A. Warrender. 1994. Measuring the elastic parameters for inverse bicontinuous cubic phases. *Biophys. Chem.* 49:1–12.

Tilcock, C. P. S., M. B. Bally, S. B. Farren, P. R. Cullis, and S. M. Gruner. 1984. Cation-dependent segregation phenomena and phase behaviour in model membrane systems containing phosphatidylserine: influence of cholesterol and acyl chain composition. *Biochemistry.* 23:2696–2703.

Tristram-Nagle, S., H. I. Petrache, and J. F. Nagle. 1998. Structure and interactions of fully hydrated dioleoylphosphatidylcholine bilayers. *Biophys. J.* 75:917–925.

Unwin, N. 1989. The structure of ion channels in membranes of excitable cells. *Neuron.* 3:665–676.

Unwin, N. 1995. Acetylcholine receptor channel imaged in the open state. *Nature.* 373:37–43.

Unwin, P. N. T., and P. D. Ennis. 1984. Two configurations of a channel-forming membrane protein. *Nature.* 307:609–613.

Waldbillig, R. C., and G. Szabo. 1979. Planar bilayer membranes from pure lipids. *Biochim. Biophys. Acta.* 557:295–305.

White, S. H. 1978. Formation of "solvent-free" black lipid bilayer membranes from glyceryl monooleate dispersed in squalene. *Biophys. J.* 23:337–347.

Wiener, M. C., and S. H. White. 1992. Structure of a fluid dioleoylphosphatidylcholine bilayer determined by joint refinement of x-ray and neutron diffraction data. III. Complete structure. *Biophys. J.* 61: 437–447.

Woolf, T. B., and B. Roux. 1996. Structure, energetics, and dynamics of lipid-protein interactions: a molecular dynamics study of the gramicidin A channel in a DMPC bilayer. *Proteins Struct. Funct. Genet.* 24:92–114.